Influence of preparative conditions on the surface structure and photoactivity of ZnS under UV/Sunlight

A thesis

Submitted in the partial fulfillment of the requirements for the award of degree of

MASTER OF SCIENCE
in
CHEMISTRY

Submitted by
Jyotsna
(Roll No. 301702017)
Under the supervision of
Dr. Bonamali Pal
Professor

School of Chemistry and Biochemistry
Thapar Institute of Engineering & Technology
Patiala-147004

July, 2019

Certificate

I hereby certify that the work presented in this thesis entitled **"Influence of preparative condition on the surface structure and photoactivity of ZnS under UV/ Sunlight "** submitted in partial fulfillment of the requirements for the award of degree of Master of Science in Chemistry submitted to School of Chemistry and Biochemistry, Thapar Institute of Engineering and Technology, Patiala is an authentic record of my own work carried out under the supervision of Dr. Bonamali Pal. The matter embodied in the thesis has not been submitted to any other Institute for the award of any other degree or diploma. Works of other authors cited in this thesis have been duly acknowledged under reference section of this thesis.

Date: 20/08/19 **Jyotsna**

This is to certify that the above statement made by the candidate is correct and true to the best of our knowledge.

Dr. Bonamali Pal
Professor
Thapar Institute of Engineering & Technology, Patiala- 147004

Acknowledgment

I would like to express my deepest gratitude to my supervisor, Dr. Bonamali Pal who has been a guiding force in my dissertation project, helping me in times of difficulty and always encouraging me to work hard and sincerely.

My sincere thanks to Dr. Amjad Ali, Professor and Head, School of Chemistry and Biochemistry, TIET for providing us a good working environment and resources in the lab.

Completion of this project would not have been possible without my PhD. mentor Miss Manpreet Kaur Aulakh. She has been my constant support during project work. I also want to acknowledge Mr. Aadil Bathla and Mrs. Sakshi Bhardwaj for their cooperation during the project. I am really thankful to my dissertation group mates, who were always willing to help me and gave their best suggestions.

My parents played a pivotal role helping me out during difficult times and were my support system throughout this work. This study wouldn't have been possible without them.

Last but not the least; I would like to thank my friends, Namrata and Reena for helping me in dealing with stress.

Jyotsna

Contents

List of Abbreviations

ZnS : Zinc Sulfide

UV: Ultraviolet

3-MPA: 3-Mercaptoproptionic acid

PVP: Polyvinyl pyrollidine

TAA: Thioacetaamide

RT: Room temperature

CV: Crystal Violet

DI: Deionized water

ZnS M1: ZnS/3-MPA/100ºC

ZnS M2: ZnS/PVP/80ºC

ZnS M3: ZnS/RT

ZnS M1 UC: ZnS M1 uncapped

ZnS Std.: ZnS standard

V_s: Sulfur vacancy

XRD: X-Ray Diffraction

DLS: Diffuse light scattering

SEM: Scanning electron microscopy

FTIR: Fourier transformation infrared spectroscopy

BET: Brunauer-Emmett-Teller (BET) Surface Area

BJH: Barrett-Joyner-Halenda (BJH) Pore Size distribution

List of Symbols

eV: Electron volt

h^+: Holes

nm: Nanometer

μm: Micrometer

min: Minutes

h: Hours

^oC: Degree Celsius

e^-: Electrons

VB: Valance band

CB: Conduction band

mg: Milligram

mM: Millimolar

Abstract

In this study, Zinc Sulfide nanoparticles were synthesized using different reaction conditions and capping agents. ZnS M1 were prepared by using 3-mercaptopropionic acid as capping agent followed by reflux at 100ºC for 6 h. ZnS M2 was prepared at heating temperature of 80ºC using capping agent polyvinyl pyrollidine. Further, ZnS M3 was prepared at room temperature under constant stirring for 4 h without any capping agent. The resultant powdered samples were characterized by XRD, UV- Visible absorption spectroscopy, photoemission spectroscopy, DLS, FTIR and BET. XRD results show the cubic type structure of all the samples with approachable lattice parameter to that of reported value (5.4 Å). Particles size calculated from Scherrer equation was found to be 2.1 nm, 10.26 nm and 2.4 nm for ZnS M1, ZnS M2 and ZnS M3 respectively. Small size of particles can also be predicted from TEM and SEM studies. The blue shift in absorption spectra of all the samples was seen which is attributed to changing surface properties with changing preparation conditions and capping agents. Nitrogen adsorption desorption analysis for all samples resembles with type IV isotherm which is characteristic peak of mesoporus nature. Specific surface area calculated from BET analysis was 252 m^2g^{-1}, 205 m^2g^{-1} and 32 m^2g^{-1} for ZnS M1, ZnS M2 and ZnS M3 respectively. Further photoactivity was also studied using crystal violet as model dye under UV and solar illumination. The study shows that changing reaction conditions and capping agent of ZnS shifts its degradation property in sunlight which is more efficient as is free of cost.

Zinc Sulfide is a II–VI type metal sulfide direct semiconductor photocatalyst with unique properties. It is a chemically stable, water insoluble and a non-toxic intreninsic n-type semiconductor. It is one of the most significant semiconductors of its type as it possesses wide band gap energy (3.5 eV for blend and 3.8 eV for wurtzite), small bohr radius, high exciton energy and comparatively high photoactivity [1]. Their different nanosized structures act as good photocatalyst for degradation of dyes, water splitting for production of H_2 and for photoreduction of CO_2 [1]. Although, ZnS is highly UV active catalyst but it is also observed to show its activity in sunlight due to the presence of UV radiation in sunlight. The absence of any toxic element in ZnS and its remarkable photocatalytic activity shows as widespread use. Thus, various efforts have been already made to make ZnS UV-Visible photoactive as well. Doping with various transition elements [2], change in its morphology [3] and capping agent are some factors which may results in shifting its photocatalytic activity towards visible region.

There is a great influence of capping agents and method of preparation over the size, shape, growth rate and optical properties of nanoparticles [4]. The functionalities of capping agent covalently bind with the surface of nanoparticles and controls their shape and size through charge transfer. Capping of organic layer over nanoparticles increases its stability, thereby resulting in much smaller size by decreasing its agglomeration and controls the crystallite properties of the material [5]. Li *et.al* [6] synthesized ZnS using EDTA as a surfactant at room temperature and its hydrophilic nature contributed to effective degradation of water soluble dyes.

Furthermore, the synthesized route for preparation of nanoparticles also affects its surface and catalytic property [7] .It is widely studied that chemical co-precipitation method is one of the easier methods to handle and produces less aggregated size controllable nanoparticles. Wageh *et.al* [8] synthesized mercaptoacetic acid capped ZnS by changing reflux time. It was observed that the position of band edge emission intensity was enhanced by increasing reflux time and defect sites were increased by lowering the duration of refluxing. Similarly, Zhang *et.al* [9] prepared ZnS using different concentration of precursors (ZnO and thiourea) resulting in enhanced degradation efficiency. The maximum efficiency was shown by 1:2 of ZnO and thiourea respectively under visible light for 3 h due to shifting of ZnS towards visible region by

the conversion of thiourea to thiocynauric acid. Sharma *et.al* [10] reported the synthesis of thioglycerol capped and uncapped ZnS and showed the effect of capping agent over band gap, crystallity, luminescence intensity and monitored the photocatalytic activity of different dyes under UV-Visible light.

Khan *et.al* [11] synthesized polyvinyl acralydine (PVA) encapsulated ZnS films by changing percentage of PVA and analyzed it by UV-Visible absorption, photoluminescence and IR studies. Catalyst with 1% PVA showed maximum degradation of methylene blue under sunlight for 660 min due to strong interaction of PVA with ZnS which resulted into increased absorption in sunlight. Waghadkar *et.al* [12] changed the reaction time using hydrothermal synthesis at 150ºC and highly efficient nanoparticles were prepared from 24h reaction time and showed effective degradation of methylene blue within 2h of solar irradiation. Moreover, Kaur *et.al* [13] used sodium dodecyl sulphate as a surfactant for preparation of ZnS by simple co-precipitation method for degradation of brilliant dye under sunlight.

2 Research Gap:

There are numerous reports in the literature for the synthesis of ZnS nanoparticles using different methods showing higher activity mainly in UV source due its higher band gap (3.54 eV) value. Moreover, metal nanoparticles are to be loaded/doped so as to activate ZnS particles [14] in visible region as well. However, few research groups have made efforts to make bare ZnS nanostructures sunlight active by using different capping agents. In this regard, ZnS was prepared under different reaction conditions and capping agents which found to be photoactive in both UV and solar irradiations due to strong interactions between functional groups of surfactant and inorganic ZnS particles.

3 Objective:

- To prepare ZnS nanoparticles using different capping agents, synthetic routes and reaction conditions.
- To study degradation of crystal violet with synthesized ZnS nanoparticles in both UV and solar light.

4 Materials and Methods:

4.1 Materials Required:

Zinc nitrate hexahydrate ($ZnNO_3.6H_2O$), Thioacetamide (C_2H_5NS), Polyvinyl pyrrolidone $(C_6H_9NO)_n$ was purchased from loba chemie. Zinc acetate ($Zn(CH_3CO_2)_2.H_2O$) and sodium sulfide (Na_2S) was purchased from s d fine-chem. limited and 3-Mercaptopropionic acid ($HSCH_2CH_2CO_2H$) was purchased from spectrochem. All the chemicals used here are of analytical (AR) grade and are used without any further purification.

4.2 Methods:

4.2.1 Preparation of ZnS/3-MPA/100ºC (M1):

In a 250 mL round-bottom flask, zinc acetate (0.878 g) was dissolved in de-ionized (DI) water (100 mL) and heated at 100ºC after the addition of 5 mL 3-mercaptopropionic acid (3-MPA) under constant magnetic stirring. In a separate beaker 50 mL aqueous solution of thioacetamide (TAA) (0.601 g) was prepared and injected into above prepared solution. The entire solution was refluxed at 100ºC for 6 h. The resulting white precipitates were washed several times with DI water and ethanol followed by drying at 60ºC for 6h [15]. Similarly, 3-MPA uncapped ZnS (ZnS M1 UC) nanoparticles were prepared without adding capping agent.

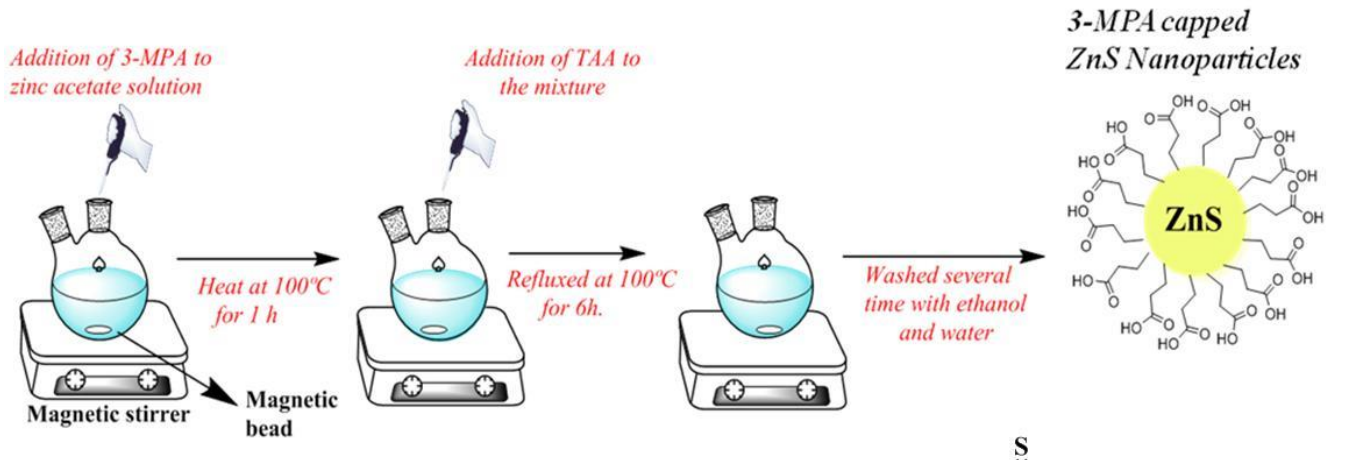

Scheme 1. Synthesis of ZnS/3-MPA/100ºC (M1)

4.2.2 Preparation of ZnS/PVP/80ºC (M2):

In 25 mL of DI water 0.06 M of zinc nitrate and PVP (2% w/v) were dissolved and the solution was set to magnetic stirring for 1 h at room temperature. To the above solution 0.4M of thioacetamide (TAA) was added. The whole solution was heated at 80ºC for 3 h with constant stirring. The precipitates were formed which were washed several times with DI water and ethanol followed by overnight drying in air [16].

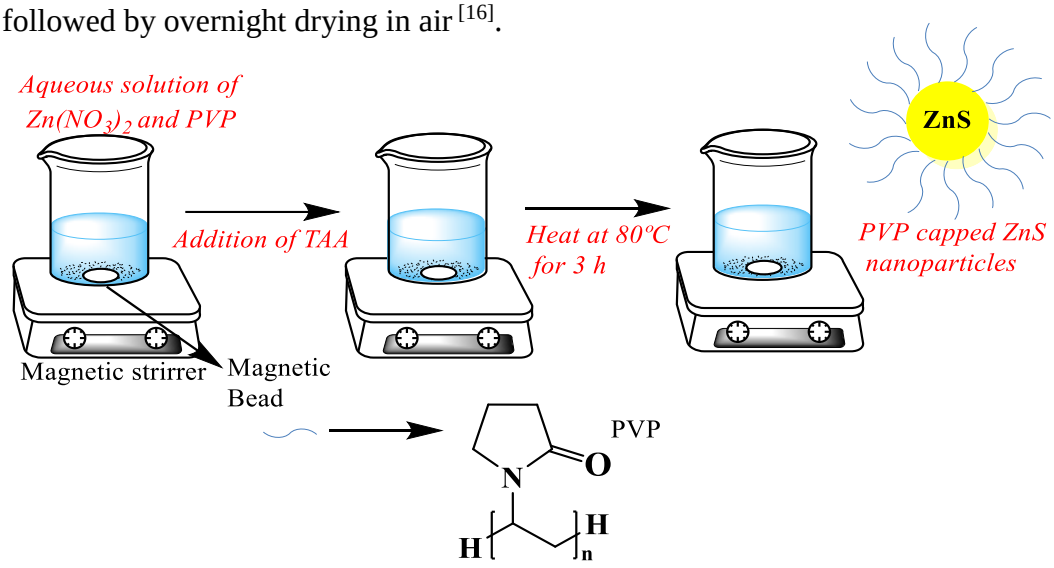

Scheme 2: Synthesis of ZnS/PVP/80ºC (M2)

4.2.3 Preparation of ZnS/RT (M3):

For synthesis of uncapped ZnS, aqueous solution of 0.01M of zinc nitrate was prepared in 50 mL of DI water. The pH of the solution was set to 10 by addition of sodium hydroxide. In a separate beaker 0.01M of sodium sulfide was prepared in 50 mL of DI water and was then slowly added to above solution.

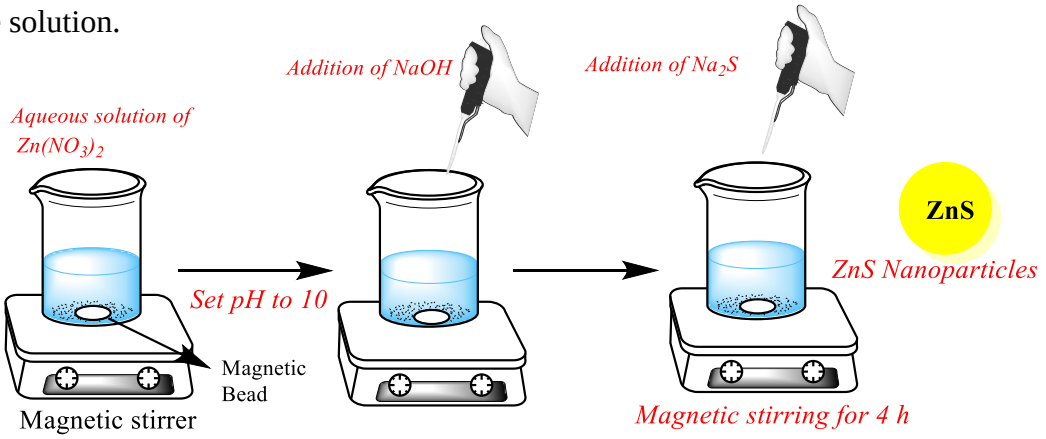

Scheme 3: Synthesis of ZnS/ RT

The whole solution was set to constant magnetic stirring for 4h. White color precipitates were formed which were washed further 3-4 times with DI water and ethanol. The precipitates were then dried at 80ºC for 6 h [17].

4.3 Characterization techniques:

- *X-ray diffraction:* This technique is used for characterizing the crystal planes, phase, structure a solid material. Further, Scherrer's equation can be applied for calculating the crystal size of solid. Herein, the analysis was done on Panlytical Xpert Pro X-ray diffractometer (powder) in SAIF Labs (Panjab University, Chandigarh) which is furnished with fast solid state detector and use Cu-Kα ($\lambda = 1.54\,\AA$) radiation for analysis.
- *UV-Visible Spectrophotometry analysis:* It helps in analyzing the optical (absorption) properties of the catalysts. On the basis of absorption peaks the size, shape, band gap, concentration and agglomeration state of nanoparticles can be estimated. Thus, it is consequently is a useful characterization technique. These absorption studies were done on Champion UV – visible spectrometer in TIET.
- *Dynamic light scattering and Zeta Potential:* Based on Brownian motion, DLS technique helps in identifying the hydrodynamic size of the material. Zeta potential helps in determining the charge over a particle which indirectly relates with the stability of the particles. The analysis was done on Malvern ZEN3600 in TIET.
- *Fluorescence spectrophotometry analysis:* Perkin Elmer LS 55(TIET) was used for determining optical and electronic properties of material. It is used to analyze surface defects of nanoparticles and change in intensity of excitation and emission spectra after capping.
- *Scanning electron microscopy and Transmission electron microscopy:* The SEM analysis has been carried out on JSM-7600 F (0.1 to 30 KV) SAI labs, Patiala and TEM analysis has been carried out from PAU, Ludhiana on Hitachi H-7650. These techniques help in determining the size and surface morphology of nanoparticles by selecting the particular area for analysis.

- *FTIR:* This technique has been used for analyzing the presence of various chemical groups over nanoparticles and nanoparticles itself. Agilent Cary-600 series (TIET) was used to carry out the analysis.
- *BET:* BET analysis is used to calculate the surface area and pore size/ value of catalyst by adsorption of gas over its surface. From obtained curve after BET analysis predication can be done regarding porosity of material. Autosorb-1, Quantachrome Instruments, USA (TIET) was used for the analysis.

4.4 Photocatalytic activity of ZnS:

2 mg of ZnS was added to 10 mL of 0.025mM CV dye in 15 mL test-tube. The solution was set to stir in dark for 60 min for attaining adsorption desorption phenomena followed by 3h illumination under sunlight and UV radiations for photocatalytic degradation. Moreover, the time scale analysis was also carried out after every 30 min for 3 h under the light source. In all the cases degradation efficiency was evaluated by observing change in absorption value on UV-Visible spectrophotometer. Schematic representation of reaction setup was represented in scheme 4.

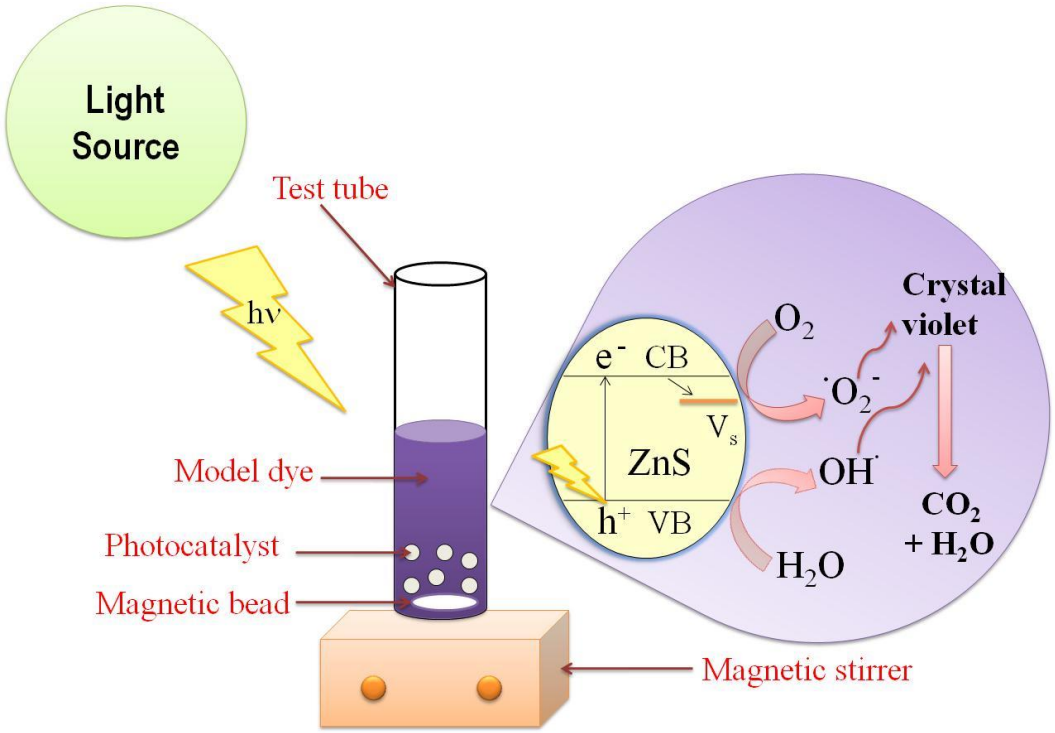

Scheme 4. Schemetic representation of reaction setup

5 Results and discussion:

5.1 Structural and optical analysis:

Fig 1 shows the UV-Visible absorption spectra of ZnS prepared from different methods and standard ZnS. This study was done by dispersing 1 mg of catalyst with help of ultrasonication (1 h) in 5 mL of water. ZnS M1 showed the absorption edge at 308 nm whereas standard ZnS showed absorption peak at 400 nm. The blue shift of ZnS M1 was attributed to quantum confinement effect. Moreover, ZnS M2 and ZnS M3 also showed blue shift with respect to standard with absorption edge at 341nm and 346 respectively whereas absorption edge was observed at 365nm for ZnS M1 uncapped which showed the role of 3-MPA in optical properties of ZnS M1.

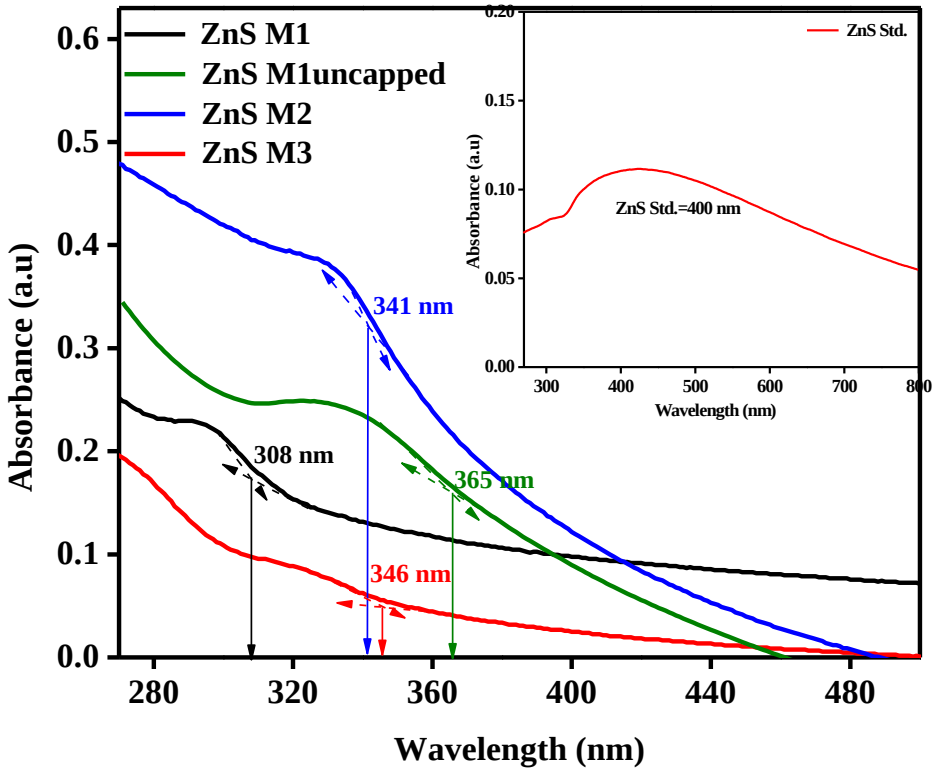

Fig 1: UV-Visible absorption spectra of ZnS M1, ZnS M2, ZnS M3, ZnS M1 UC and ZnS Std.

Structural analysis of synthesized ZnS was carried out using XRD. Fig. 2 shows XRD of ZnS prepared from method M1, M2 and M3. ZnS prepared from method M1 showed three diffraction peaks at 2θ 28.45º, 47.63º and 56.26º with corresponding planes (111), (220), and (311). Similarly, ZnS M3 showed three peaks along 2θ 28.91º, 47.58º and 56.67º with similar planes as that of ZnS M1. Further ZnS M2 showed peaks along 2θ 28.71º, 33.26º, 47.73º,

56.66º, 59.44º, 69.53º and 76.86º. The peaks are attributed to planes (111), (200), (220), (311), (222), (400) and (331) and showed cubic structure with computed average lattice parameter of 5.40 Å, 5.39 Å, and 5.38 Å which was approachable to reported value of 5.40 Å [18].

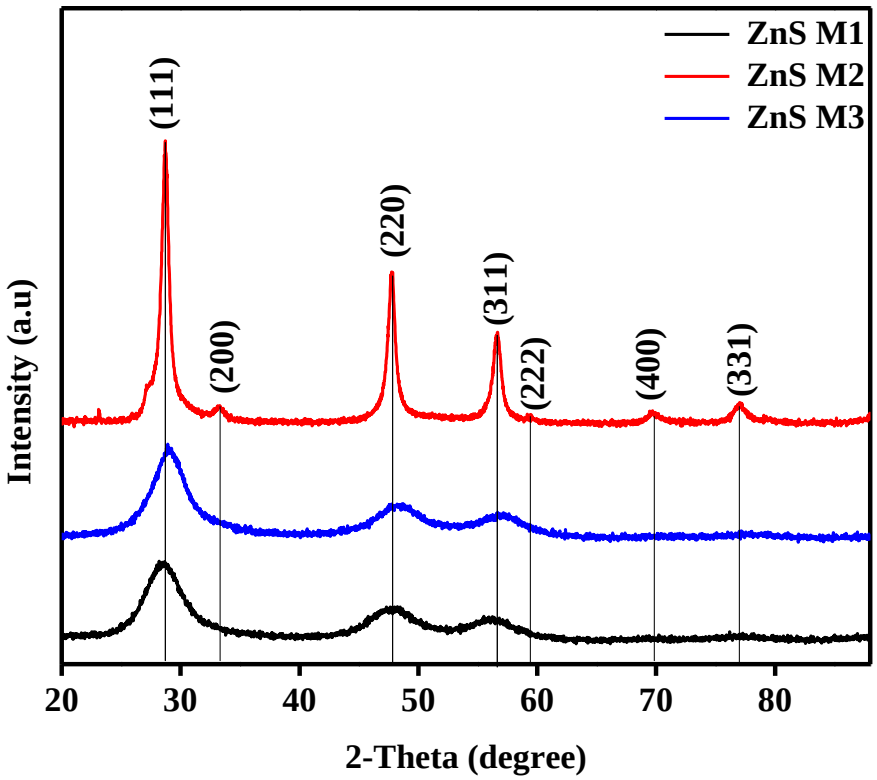

Fig 2: XRD pattern of ZnS/MPA/100ºC (M1), ZnS/PVP/80ºC (M2) and ZnS/RT (M3)

In case of PVP capped ZnS diffraction peak at 2θ 27º is attributing to wurtzite phase or stacking defect in ZnS [16]. The various crystal planes along different angles obtained matches (JCPDS NO. 05-0566) [15]. The average particle size of ZnS M1, ZnS M2 and ZnS M3 calculated from Scherrer equation $D=K\lambda/d\cos\theta$, (here, d is the particle size, λ=.154 nm (Cu), K=crystalline shape factor (0.9), d=FWHM, θ=angle in radian) is 2.10 nm, 10.26 nm and 2.40 nm respectively.

The DLS analysis was carried out to estimate the hydrothermal size (Fig 3(a)) of all nanoparticles which was found to be 266 nm, 1.4 µm, 297 nm, 567 nm and 1.2 µm for ZnS M1, ZnS M1 UC, ZnS M2, ZnS M3 and ZnS Std. respectively. Further the zeta potential was also carried in order to find the charge over surface of the particles as shown in Fig 3(b). The highest charge of -23 mV was observed in case of ZnS M1 which co-related its higher stability in comparison to other catalysts.

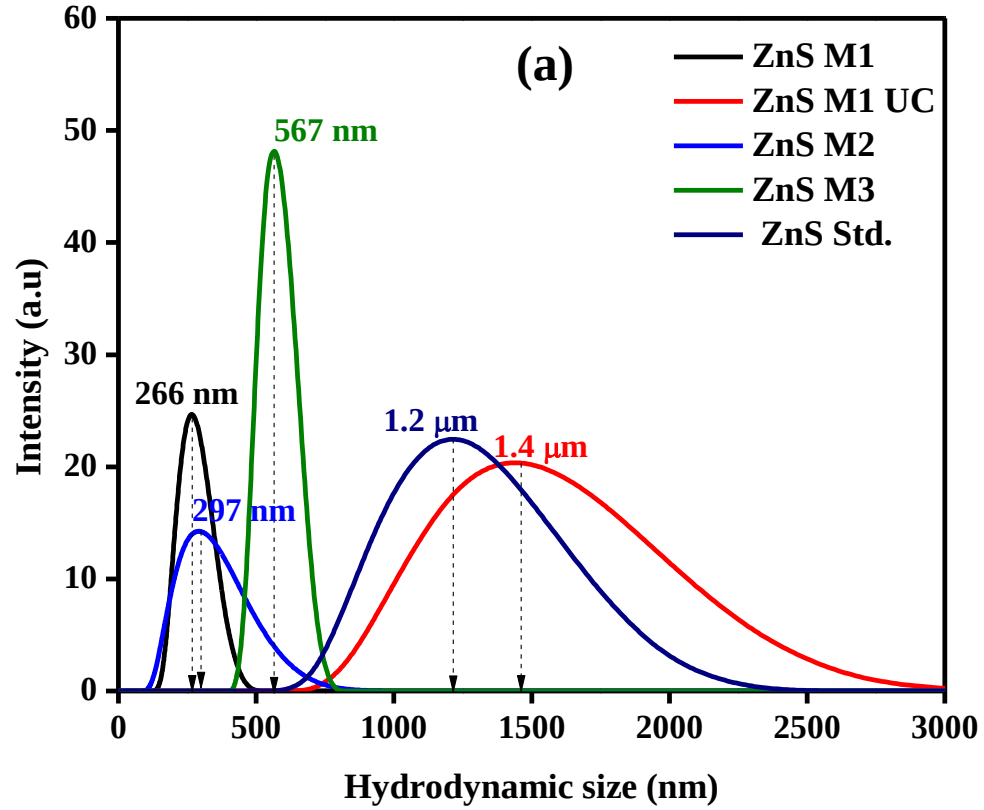

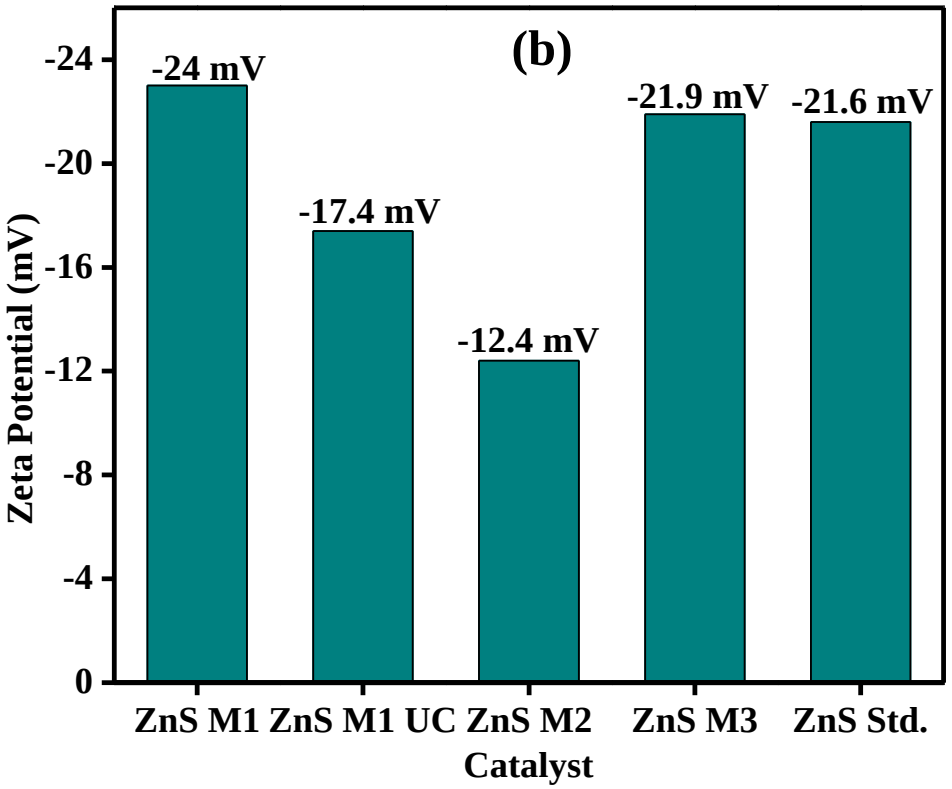

Fig 3(a): Hydrodynamic size and (b) zeta potential of ZnS M1, ZnS M2, ZnS M3, ZnS M1 UC and ZnS Std.

TEM and SEM images of ZnS depicted below in Fig 4(a) and Fig 4(b) respectively showed the small size of nanoparticles in case of both ZnS M1 and ZnS M2. Both TEM and SEM images of particles showed agglomeration of particles.

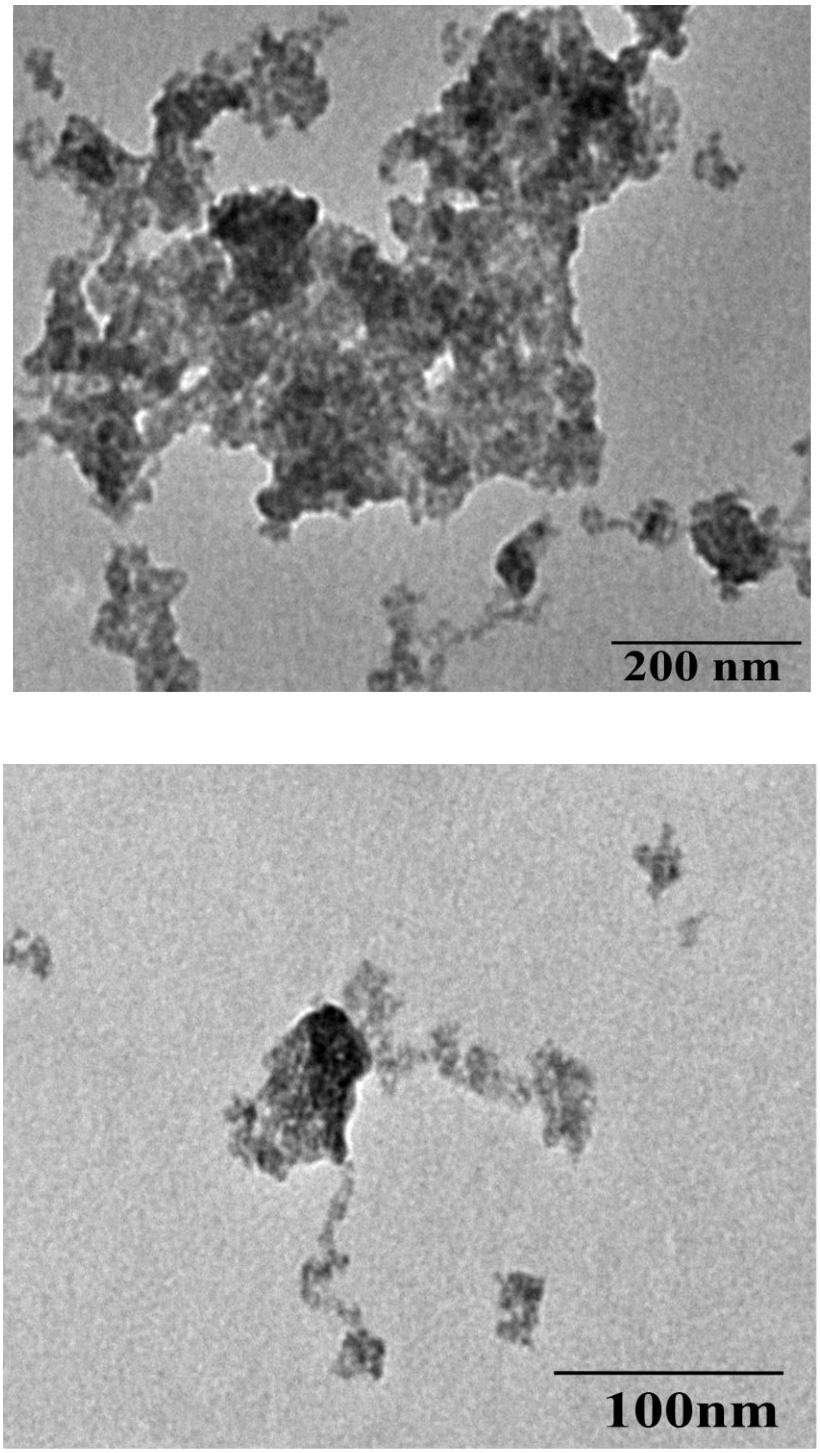

Fig 4(a): TEM images of ZnS M1

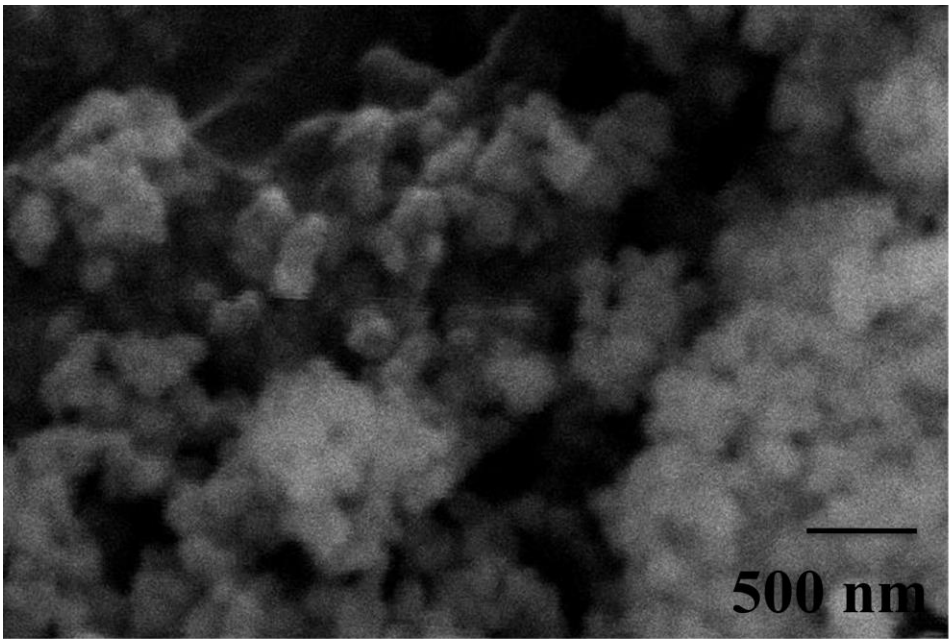

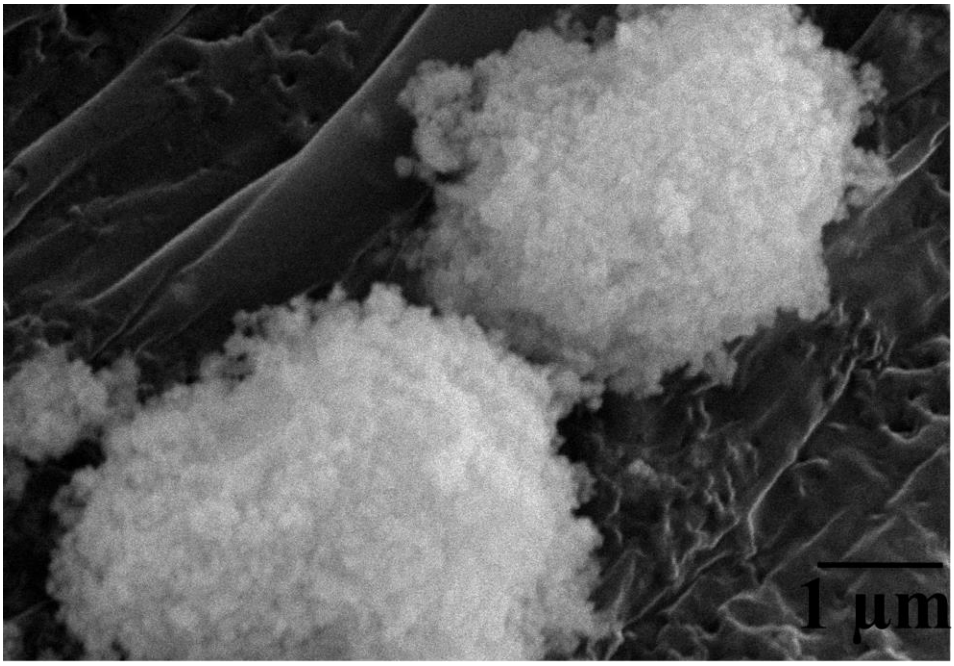

Fig 4(b): SEM images of ZnS M2

S analysis Fig 5(a), 5(b) and 5(c) shows the presence of zinc, sulfur along with oxygen. The presence of less percentage of sulfur in all cases showed the presence of sulfur vacancies.

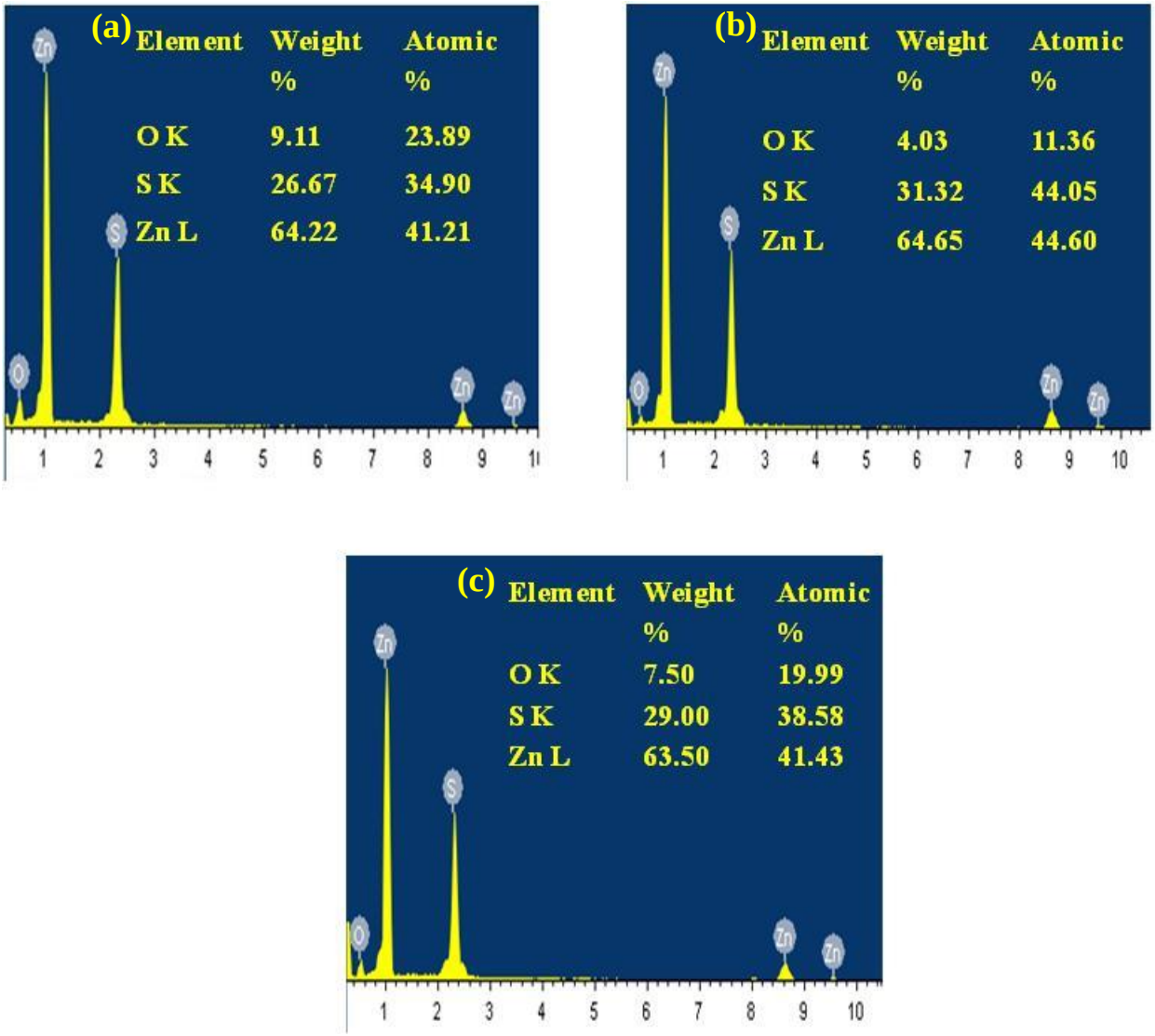

Fig 5(a): EDS spectra of ZnS M1 5(b) ZnS M2 and 5(c) ZnS M3

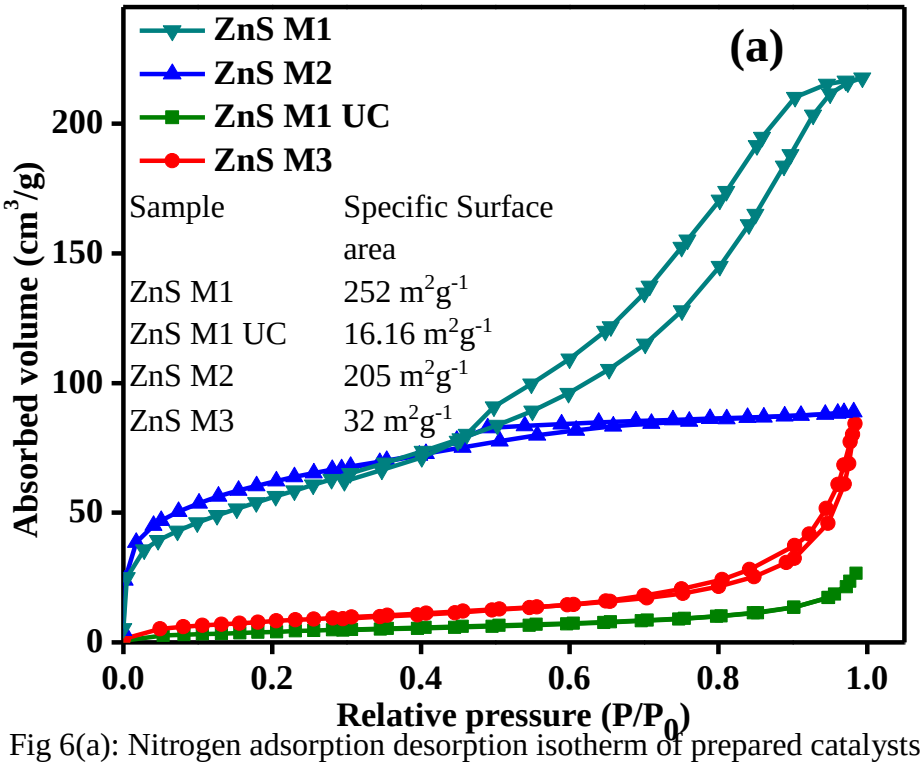

Fig 6(a): Nitrogen adsorption desorption isotherm of prepared catalysts

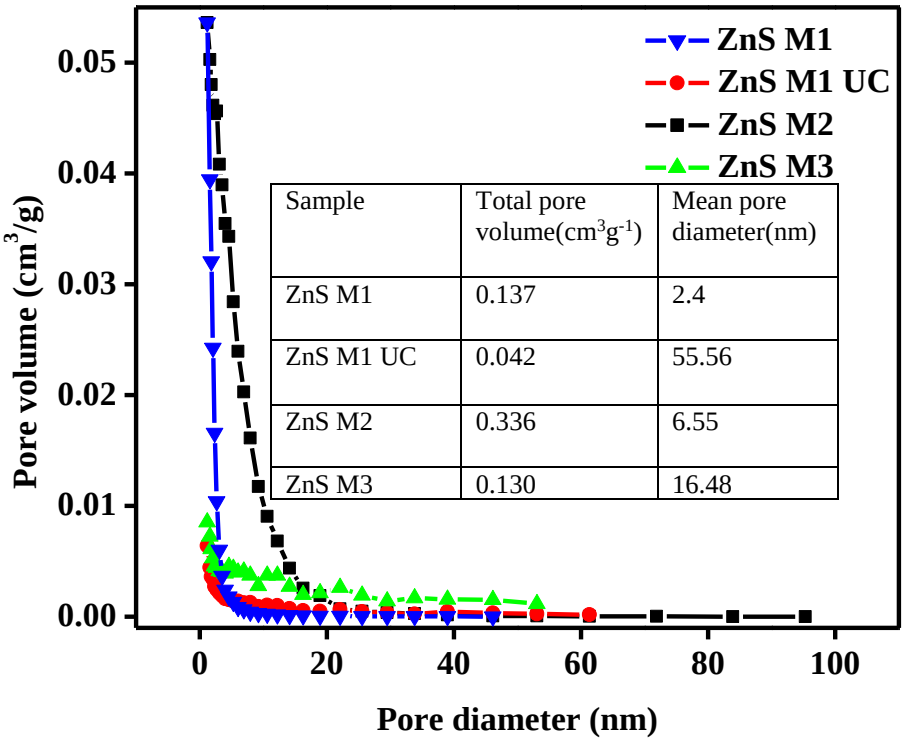

Sample	Total pore volume(cm^3g^{-1})	Mean pore diameter(nm)
ZnS M1	0.137	2.4
ZnS M1 UC	0.042	55.56
ZnS M2	0.336	6.55
ZnS M3	0.130	16.48

Fig 6(b): Pore size distribution curves of prepared catalysts

Furthermore, Brunauer-Emmett-Teller (BET) characterization showed nitrogen adsorption and desorption isotherms of samples which followed type IV isotherms and depicted the mesoporous nature of the samples as shown in Fig 6(a). ZnS M1 resulted in highest surface area of 252 m^2/g (Fig 6(a)) with mean pore diameter of 2.44 nm depicting the presence of 3-MPA as

in comparison to the 3- MPA uncapped ZnS showed lower surface area of 16.16 m^2g^{-1}. BJH curves of all samples in Fig 6(b) resulted in maximum pore size distributions in 0 nm-15 nm range

Fig 7 depicted photoemission spectra of prepared ZnS catalysts at fixed excitation wavelength of 320nm. Samples were prepared in same manner as that for UV-Visible absorption all samples showed luminescence in visible region except the standard ZnS because of vacancy defects. Emission at around 420 nm is known from sulfur vacancies [19]. Other emission can be attributed to electron transfer from different sulfur vacancy to zinc vacancy.

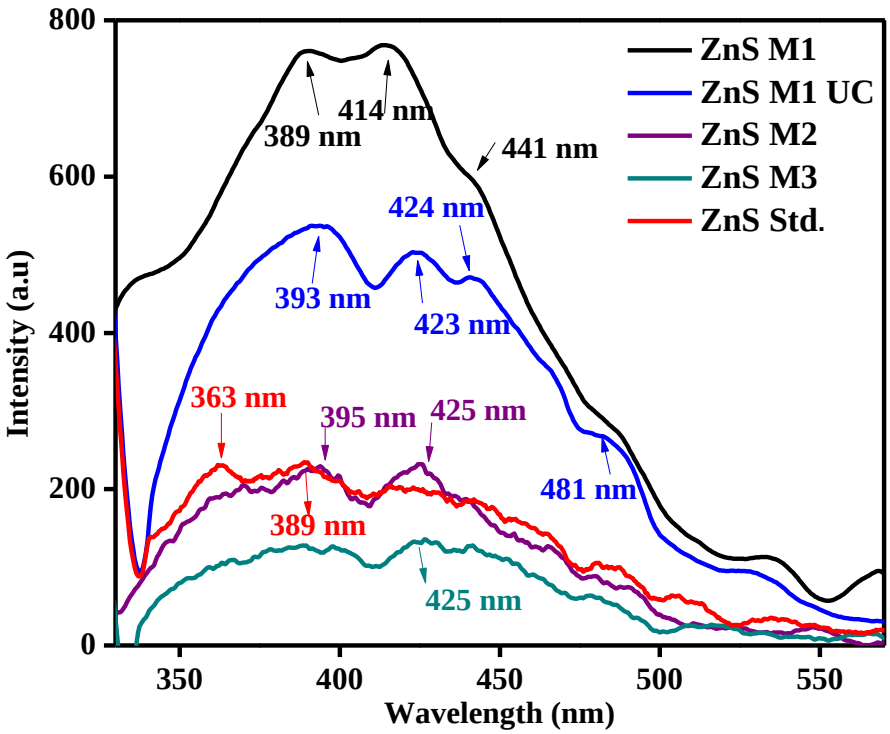

Fig 7: Photoemission spectra of ZnS M1, ZnS M2, ZnS M3, ZnS M1 UC and ZnS Std.

Fig 8 represents the FTIR spectra of commercial available and prepared ZnS particles. A broad peak in the region 3600-3000 cm^{-1} in all cases was attributed to the presence -OH group in water as well as acid in case of ZnS M1. In case of ZnS M1 strong peaks at 1549 and 1357 cm^{-1} showed the presence of acidic group –COOH on ZnS surface [14] whereas peak at 1607 cm^{-1} belonged to O-H stretching vibration and H-O-H bending vibration of water in case of ZnS M1 UC [11]. ZnS M2 showed transmission at 1284, 1429 and 1650 cm^{-1} for C-N and C=O of PVP[12] .ZnS M3 showed similar peak at 1570 cm^{-1} as that of ZnS M1 UC because of water. Moreover peaks at 1084 and 669 cm^{-1} are characteristics peaks of ZnS [20].

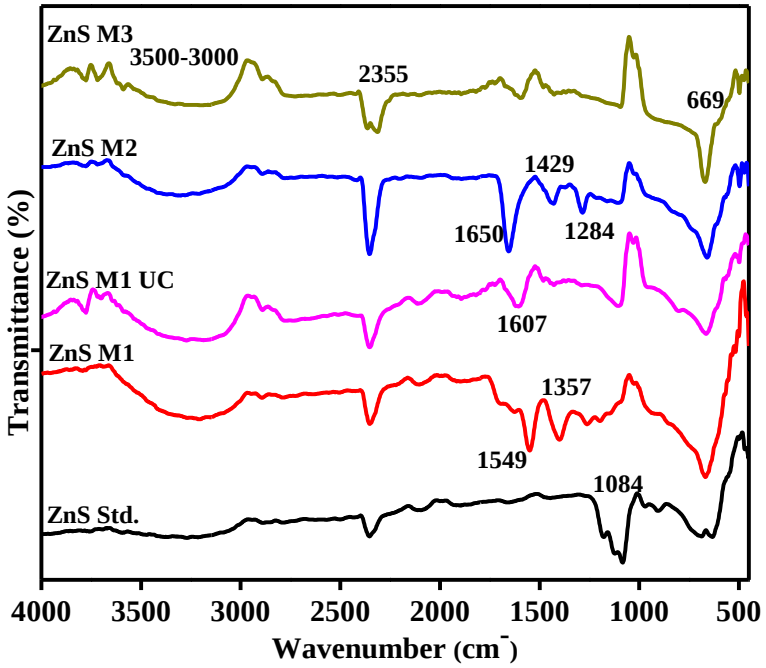

Fig 8: FTIR spectra of ZnS M1, ZnS M2, ZnS M3, ZnS M1 UC and ZnS Std.

5.2 Photocatalytic degradation study:

The photocatalytic activity was monitored by degradation of crystal violet. The calibration graph (Fig 9) was plotted between different dye concentration (0.010 mM, 0.015 mM, 0.020 mM and 0.025 mM) versus its absorbance. It helped in calculating the absorbance of unknown concentration of dye following Beer Lambert law.

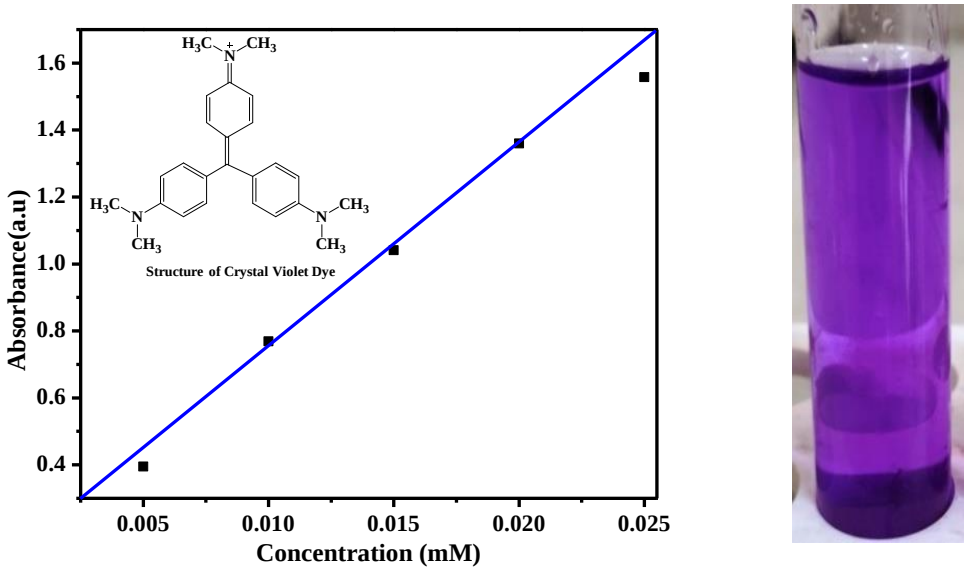

Fig 9: Calibration graph of crystal violet and its color

Fig 10(a), 10(b) and 10(c) depicted the photocatalytic degradation of CV dye in the presence of UV light with gradual increase of time with catalyst ZnS M1, ZnS M2 and ZnS M3 respectively. The absorbance value in case of ZnS M1 almost approaches to zero (Fig 10(a)) thereby showing 93% of degradation and the blue shift obtained here can be attributed to some intermediates formation. In comparison ZnS M1, the absorbance values of ZnS M2 and ZnS M3 were higher (Fig 10(b) and 10(c)) resulting in less degradation efficiency of 86% and 85% respectively. The similar results can also be predicted from color change observed for ZnS M1as shown in Fig 11(a) and 11(b).

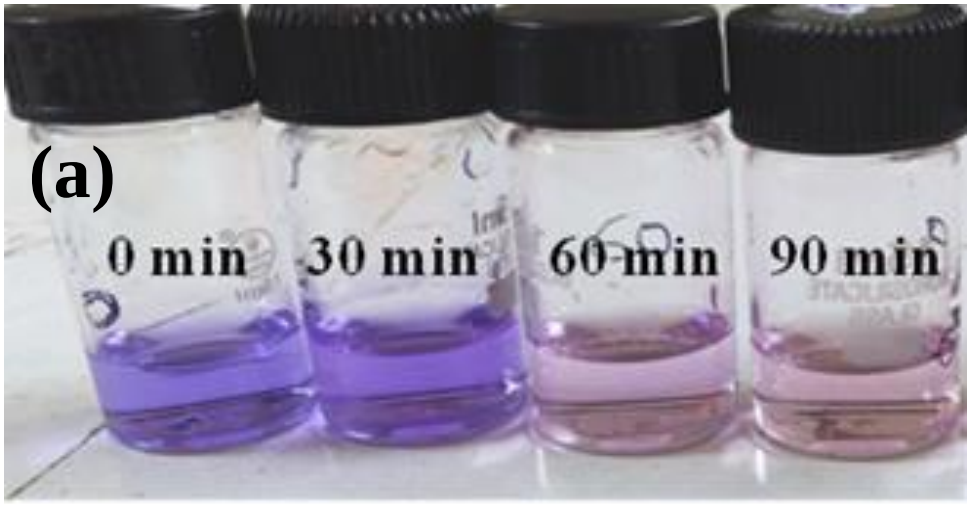

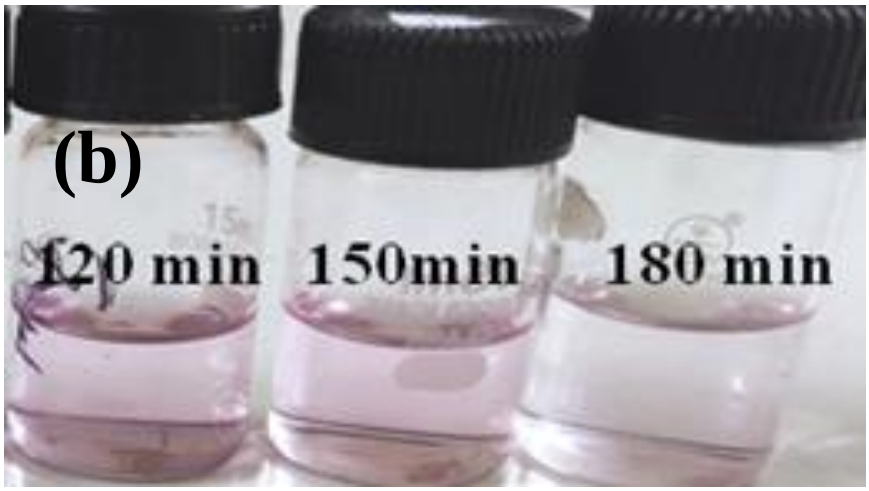

Fig 11(a): Change in color of the dye under UV light with ZnS M1 upto 90 min and 11(b) after 90 min

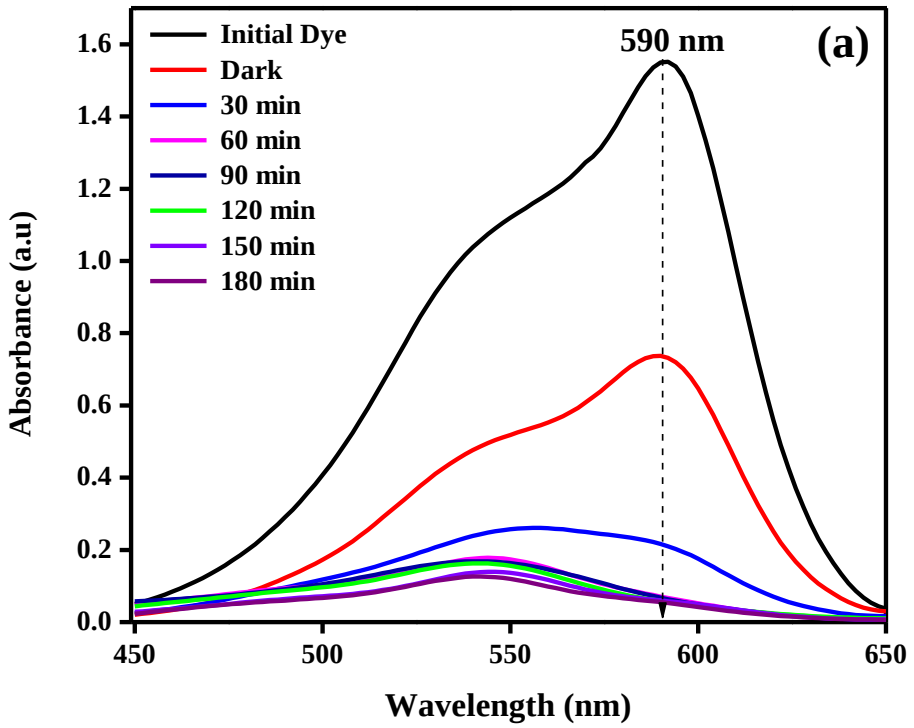

Fig 10(a): Change in absorption spectra of dye with time using ZnS M1 under UV light

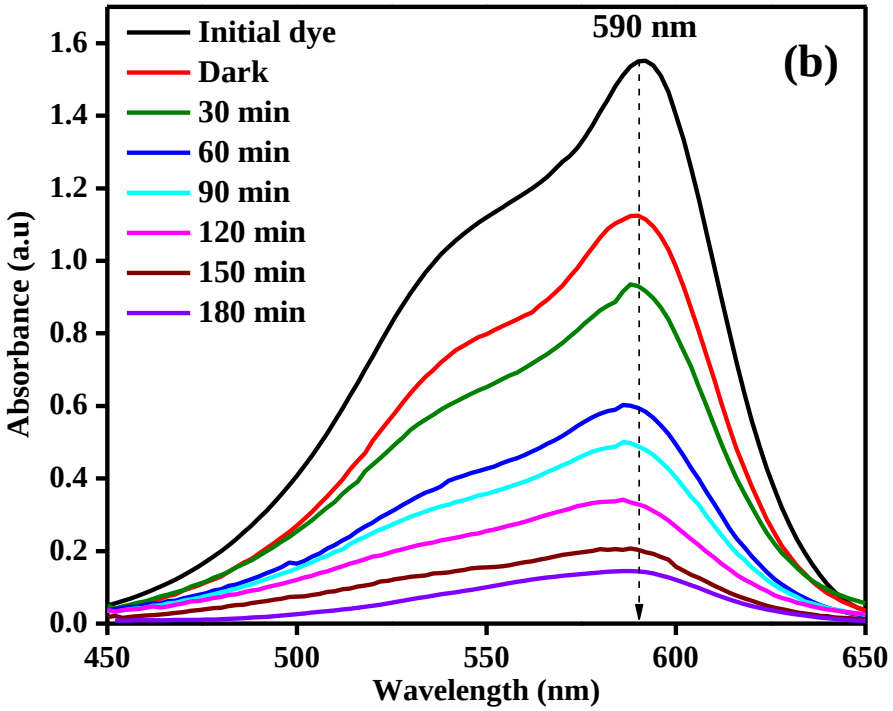

Fig 10(b): Change in absorption spectra of dye with time using ZnS M2 under UV light

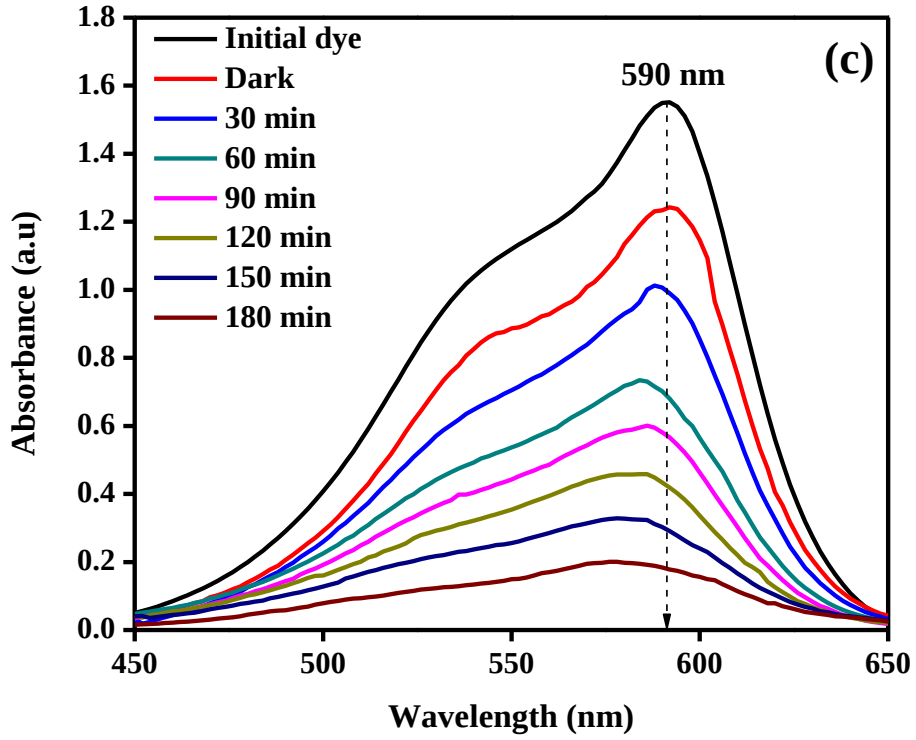

Fig 10(c): Change in absorption spectra of dye with time using ZnS M3 under UV light

Kinetic Study:

A comparative study of CV degradation from prepared catalyst as well as from ZnS Std. was performed with changing reaction time under UV light irradiation. Time course plot (Fig 12(a)), where C and C_0 are concentration after time t and initial concentration of dye, showed almost approachable degradation of CV dye at 180 min with all the catalysts however at 90 min clear difference can be seen with degradation percentage of 91%, 56% and 53% respectively for ZnS M1, ZnS M2 and ZnS M3. In comparison to the prepared catalysts, ZnS Std. showed low degradation value of 48%. The order of reaction was checked by fitting the values of concentration change into different order plots. The linear fit (R^2) values for different ZnS nanoparticles suggested that ZnS M1 best matches with pseudo second order (Fig 12(c)) where C is change in concentration with changing time t ($t/C=(1/kC_0^2)+t/C_0$) while all others followed first order reaction with equation ($-\ln C/C_0=kt$) (Fig 12(b)).

The rate of degradation under UV, k for ZnS M1 was found to have maximum value of 9.2×10^{-1} min^{-1} following pseudo second order. While the values for ZnS M2, ZnS M3 and ZnS Std. were found to be 5.4×10^{-3} min^{-1}, 4.7×10^{-3} min^{-1} and 4.3×10^{-3} min^{-1} following first order of

reaction respectively. The change in the values of rate of degradation and order of reaction can be attributed to the surface properties of the catalysts by changing the method of preparations.

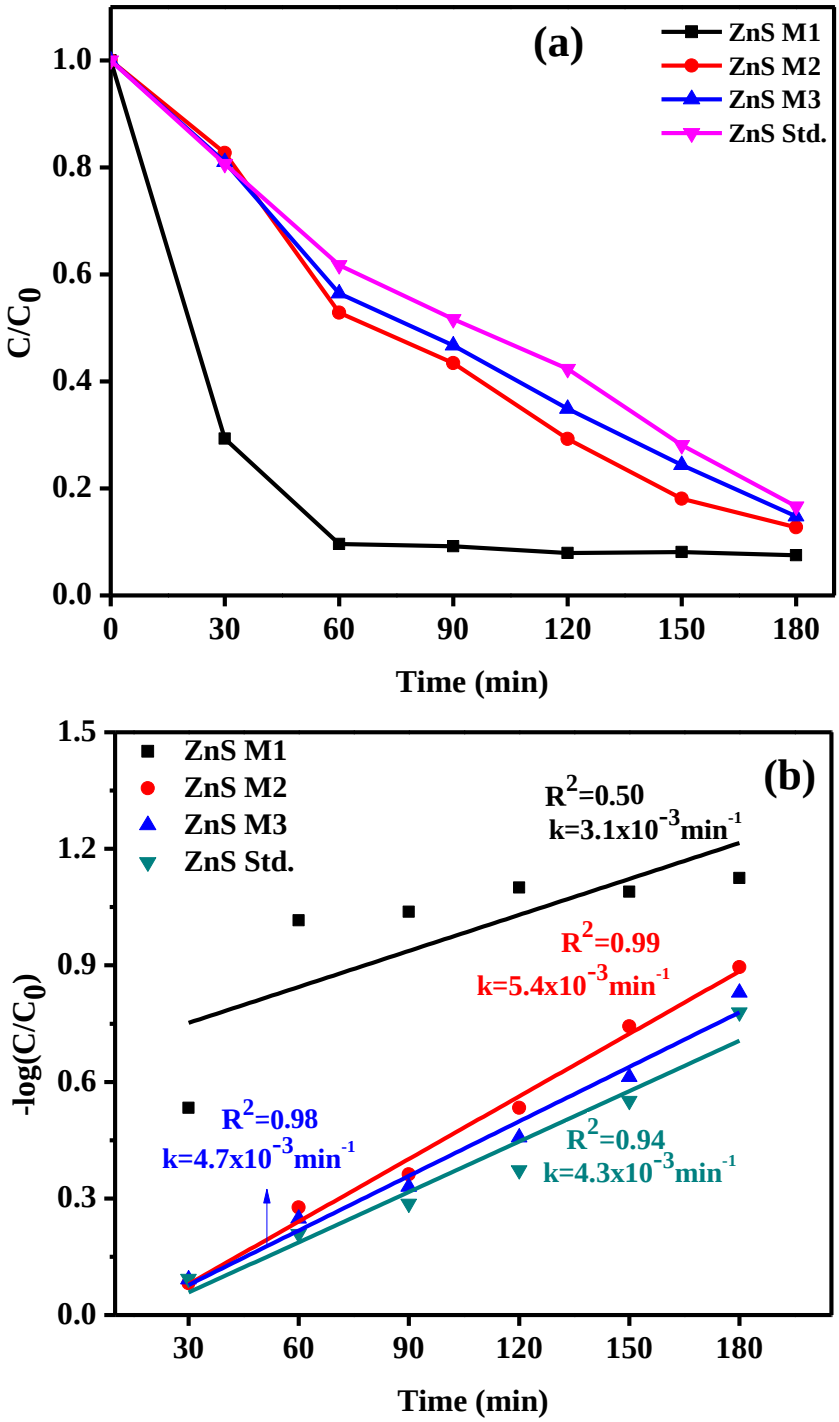

Fig 12(a): Time course plot and 12(b) first order kinetics for degradation of dye under UV light

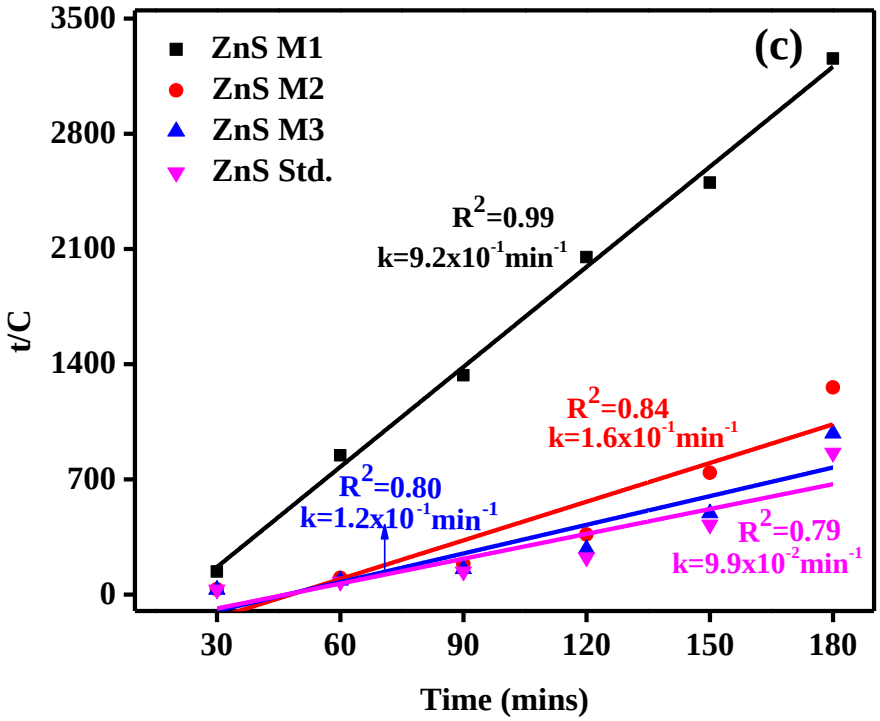

Fig 12(c): Pseudo second order kinetic Model for dye degradation under UV light

Sunlight contains 3% of UV light along with heat energy which favored degradation of reaction. In general every 10 degree rise in temperature doubles the rate of reaction. Also, strong interaction of ZnS with capping agent as well as the vacancy levels created in between energy levels favored the dye degradation in visible region [13]. Therefore, the similar manner reaction was carried out under sunlight following same reaction condition in order to check the effect of various reaction condition over ZnS. Fig 13(a), 13(b) and 13(c). Shows UV-Visible absorption graph of CV dye degradation under sunlight irradiation with catalyst ZnS M1, ZnS M2,and ZnS M3. The decrease in absorbance value with degradation is maximum for ZnS M1 though it doesn,t approaches to zero as in case of ZnS M1 in UV illimunation

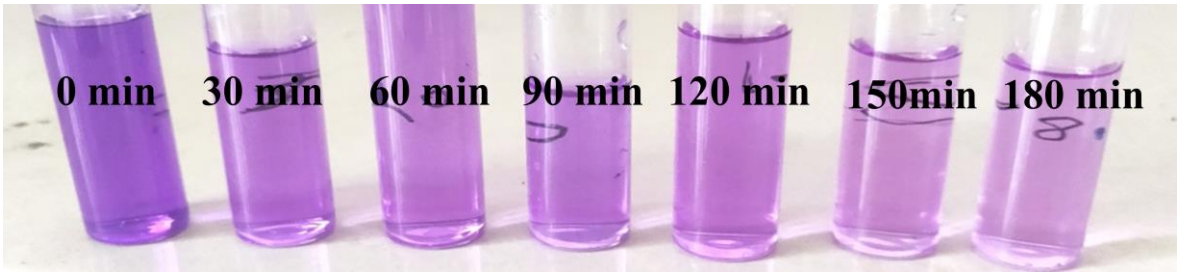

Fig 14: Change in color of dye under sunlight using ZnS M1

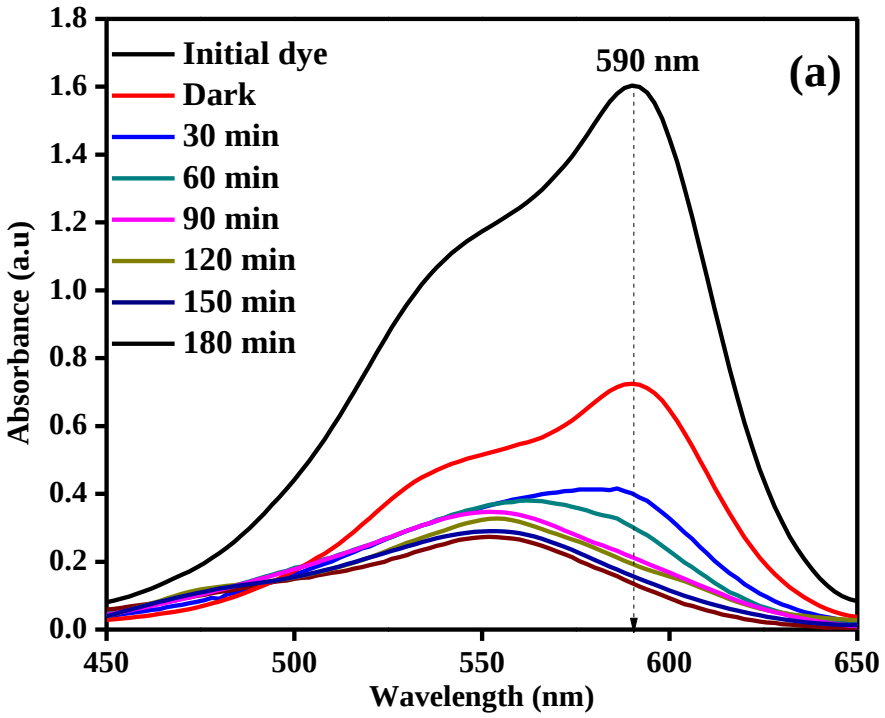

Fig 13 (a): Change in absorbance spectra of dye with time using ZnS M1 under sunlight

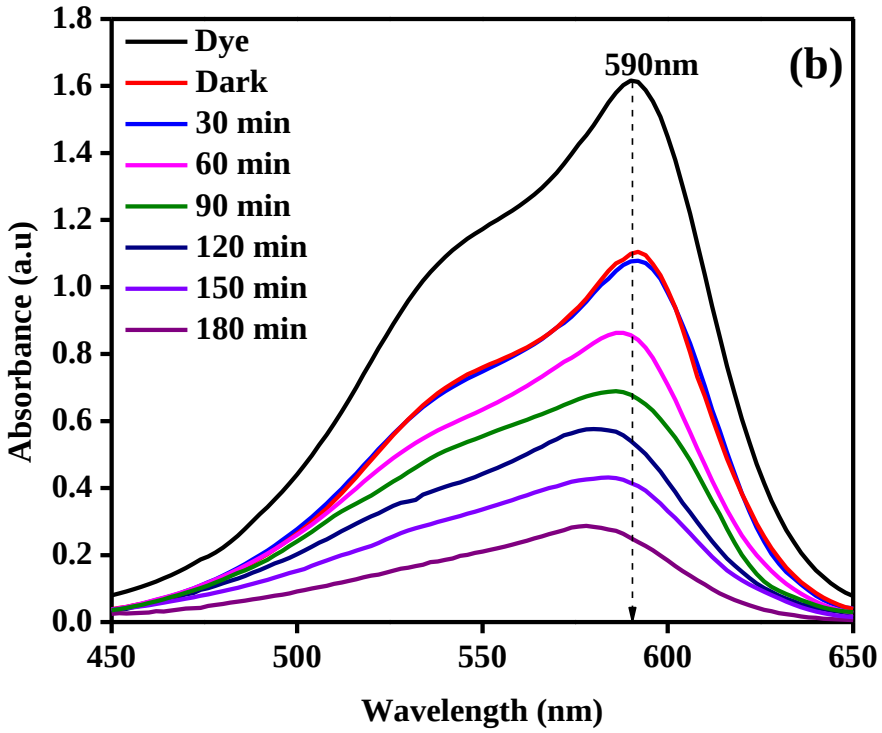

Fig 13(b): Change in absorbance spectra of dye with time using ZnS M2 under sunlight

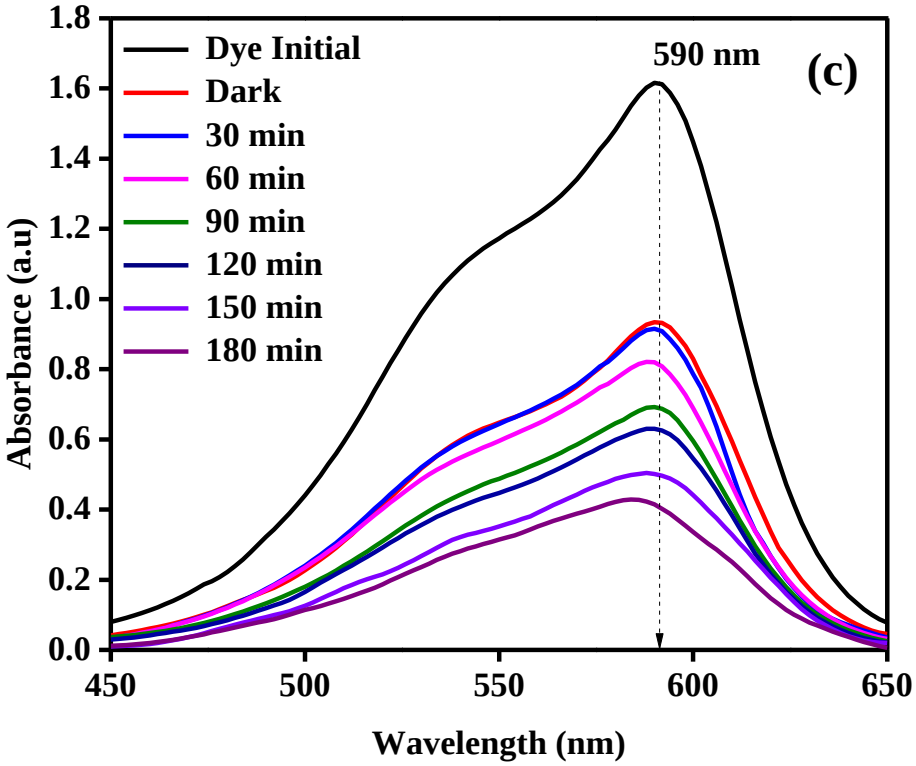

Fig 13(c): Change in absorbance spectra of dye with time using ZnS M3 under sunlight

Kinetic Study:

The comparative study for degradation of CV was studied using time course plot showed in Fig 15(a). ZnS M1 showed maximum degradation efficiency of 82% under sunlight which is low in comparison to 91% degradation under UV light. The increased degradation under UV light is because of its high energy whereas degradation under sunlight is attributed to strong interactions of 3-MPA with ZnS and sulfur vacancies levels. Also, the heat energy from sun contributed in increased rate of degradation. ZnS M2 showed approachable degradation 77% whereas ZnS M3, ZnS M1 uncapped and ZnS showed less degradation efficiency in sunlight.

Fig 15(b) and Fig 15(c) showed first order and pseudo second order kinetics of photodegradation reaction under sunlight. ZnS M1 is following pseudo second order reaction and other catalysts following first order which is similar to that under UV light. Further, for analyzing the role 3-MPA in case of ZnS M1, ZnS M1 uncapped was also prepared showing surface area of 16.16 m^2g^{-1}.

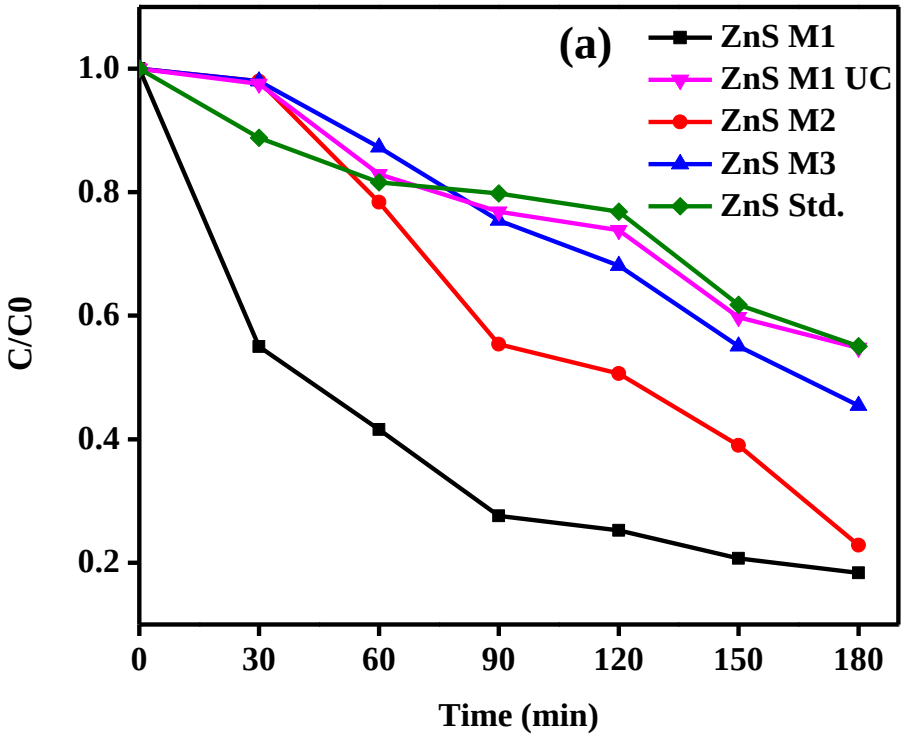

Fig 15(a): Time course plot under solar illumination

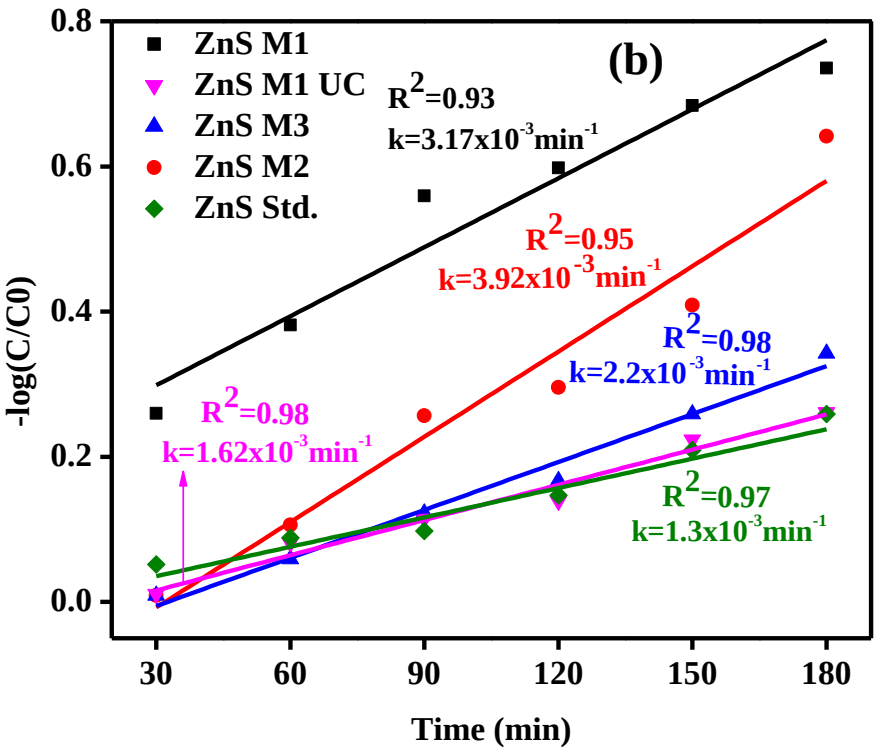

Fig. 15(b): First order kinetics for degradation under solar illumination

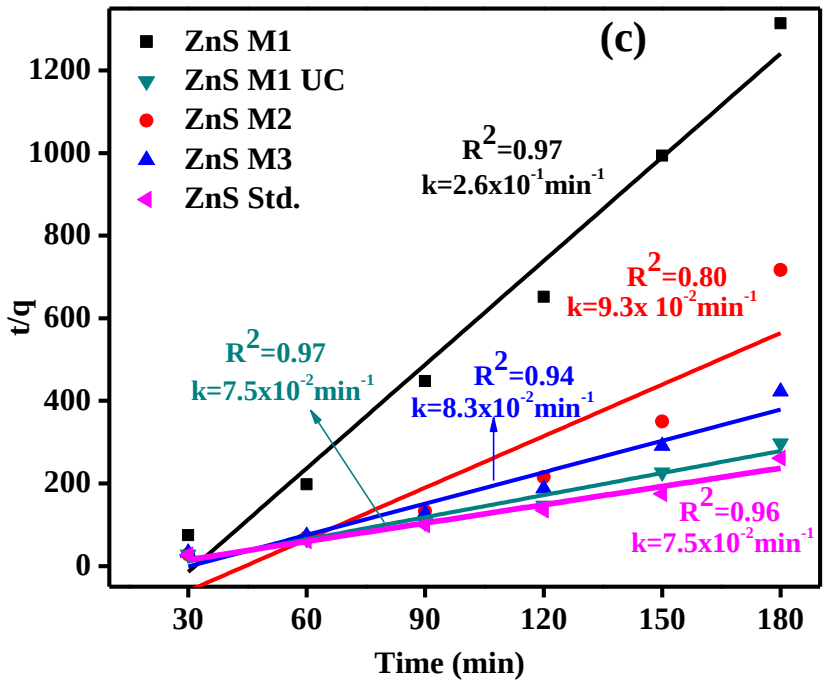

Fig 15(c): Pseudo second order kinetics for degradation under solar illumination

Kinetic study of ZnS M1 uncapped was also studied under sunlight. Rate of degradation for ZnS M1 was found to be maximum (2.6 x 10^{-1} min^{-1}) following pseudo second order reaction. Furthermore ZnS M2, ZnS M3, ZnS M1 uncapped and ZnS Std. followed first order reaction as can be depicted from linear fit curve. ZnS M2, ZnS M3, ZnS M1 uncapped and ZnS Std. resulted in with rate values of 3.92x10^{-1} min^{-1}, 2.2x10^{-1} min^{-1}, 1.62x10^{-3} min^{-1} and 1.3x$10^{-3}$$min^{-1}$ respectively

Photocatalytic mechanism of crystal violet using ZnS:

Zinc Sulfide absorbs light from UV source or sunlight and results in production of electrons and holes. The holes produced in valance band and electrons move to conduction band. H_2O and O_2 present in solution absorb over catalyst surface. At valance band, photooxidation occur which results in production of $OH^{\bullet}$ free radical. At conduction band photoreduction occurs which reduce oxygen to superoxide radical. This superoxide further produces hydrogen peroxide after oxidized by holes and H_2O_2 dissociate into $OH^{\cdot}$ free radical. This free radical degrades dye into minerals [21] as shown in scheme 4.

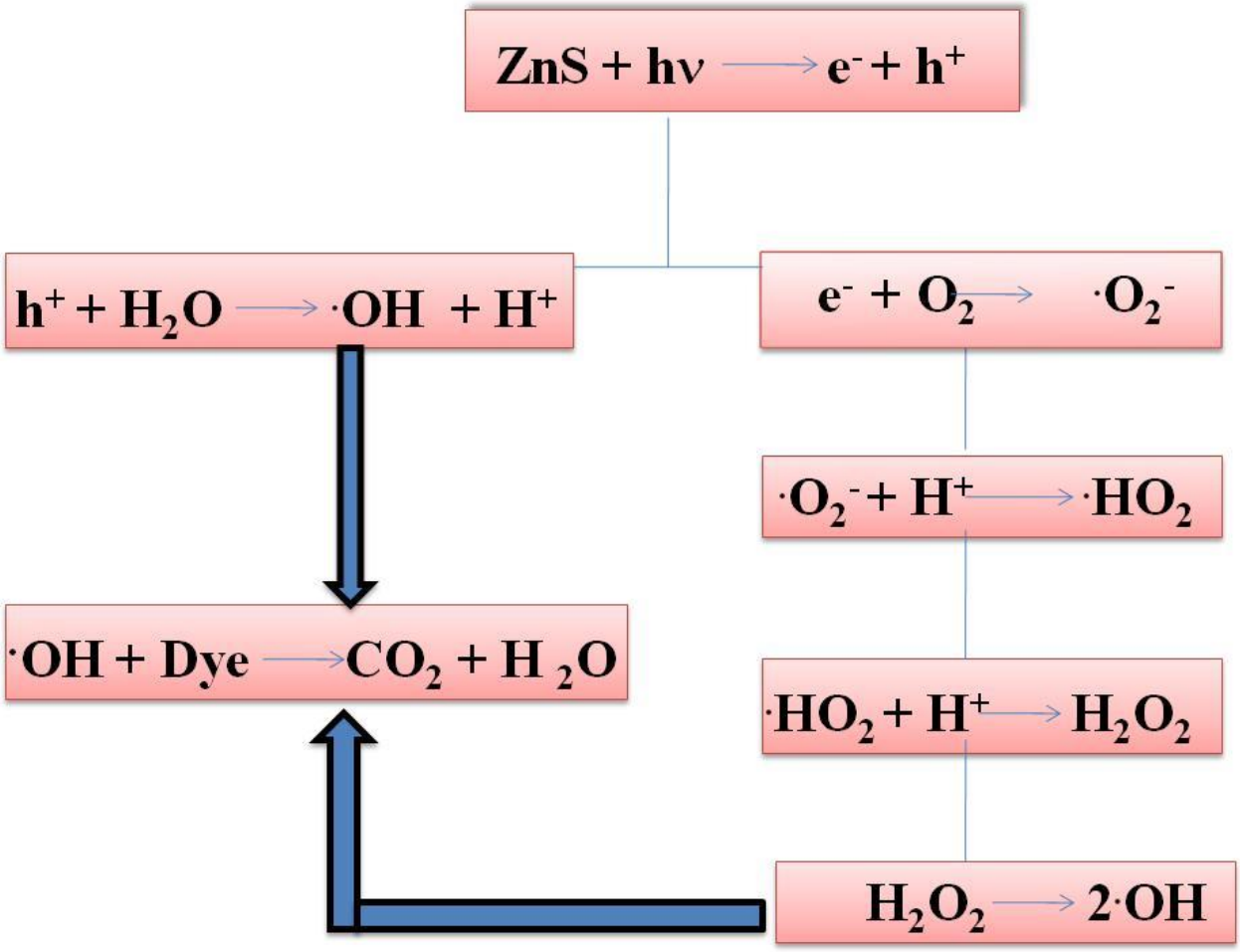

Scheme 4: Photodegradation mechanism

Fig 16 (a) and (b) showed the change in degradation efficiency by changing reaction time under UV and solar illumination for 90 min. The results depicted that ZnS M1 degraded CV with highest efficiency of 91% in 90 min under UV whereas ZnS M2, ZnS M3 and ZnS Std. showed 56% 53%, 48% degradation respectively. After 90 min of degradation ZnS M1 doesn't show much change in further degradation capacity while as ZnS M2 and ZnS M3 didn't attain more than 85 % of degradation even after 180 min. The other nanoparticles (ZnS M2, ZnS M3 and ZnS Std.) shows comparable amount of degradation. Similar trend was obtained under solar illumination as well.

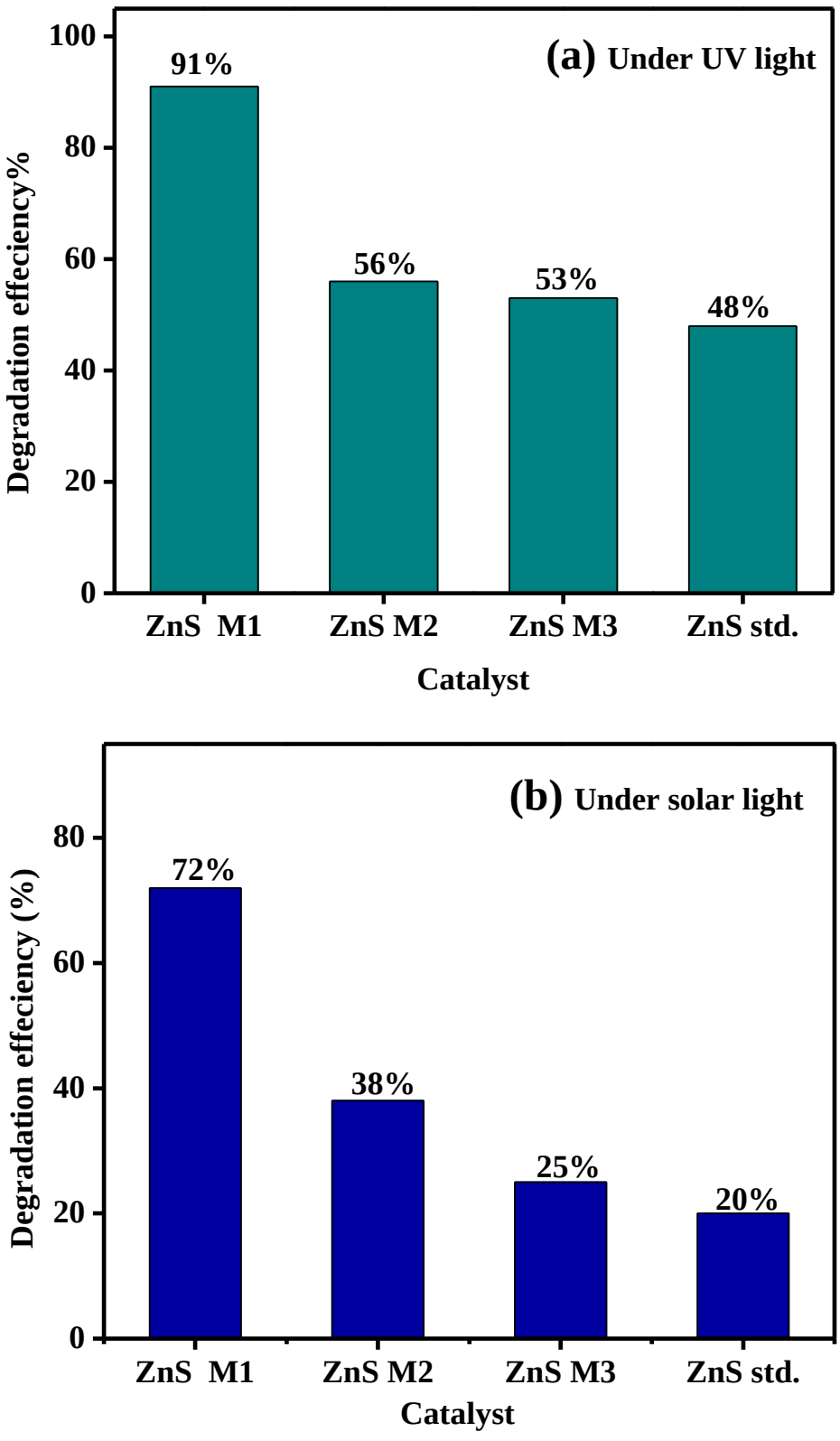

Fig. 16 (a) and 16(b): Comparison of degradation efficiency of catalysts after 90 min

A comparative bar graph (Fig 17) showed percentage degradation of CV with prepared nanoparticles under both UV and sunlight for 180 min. The maximum degradation efficiency was observed for ZnS M1 followed by degradation efficiency of ZnS M2, ZnS M3 and ZnS Std. ZnS M1shows the degradation efficiency of 91% and 72% in UV and solar illumination respectively.

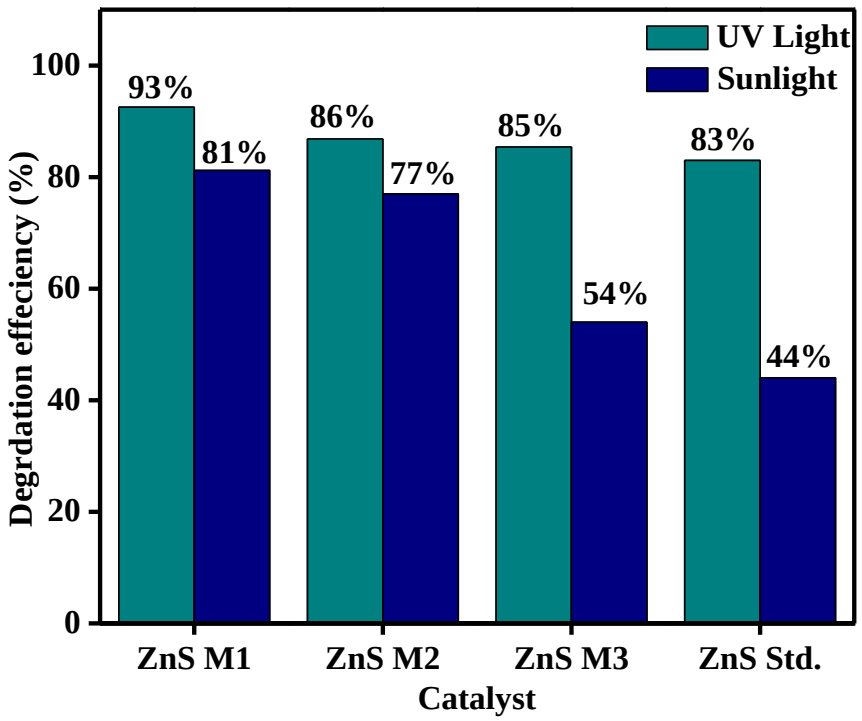

Fig 17: Comparison between degradation efficiency of catalysts under UV and sunlight

6 Conclusion:

ZnS nanoparticles modified with various capping agents was prepared in different reaction conditions using chemical precipitation method. Effect of capping agent and reaction conditions over ZnS nanoparticles was studied thoroughly by using UV-Visible absorption spectroscopy, photoluminescence spectroscopy, XRD analysis and DLS. Results reveal the blue shift in absorption edge with emission peak in visible region in all cases. XRD studies account for cubic structure with lattice parameter of about 5.4 Å. Highest zeta potential of ZnS M1 with surface area 252 m^2g^{-1} shows its good stability. Presence of 3- MPA and PVP capping over ZnS was confirmed by FTIR. EDS analysis reveals the presence of sulfur vacancy which account for good degradation efficiency in UV as well as solar light. ZnS M1 formed nanoparticles and spherical type morphology was observed for ZnS M2.

ZnS M1 showed degradation percentage of 93% and 72% in UV and solar irradiation and follows pseudo second order kinetics. After 180 min of degradation all catalysts showed approachable degradation efficiency whereas initially ZnS M1 shows degradation efficiency of 91 % in 90 min only. ZnS M1 UC showed only 44% of degradation which reveals the role of capping agent in preparation method. Higher rate of degradation in case of ZnS M1 may be due to strong interactions of ZnS with 3-MPA which increased the absorbance capacity of ZnS as well as the more sulfur vacancy levels in comparison to ZnS.

7 References:

1. Lee, G. H.; Wu, J. J., Recent developments in ZnS photocatalysts from synthesis to photocatalytic applications. *Powder Technol.* **2017**, *318*, 8-22.
2. Eyasu, A.; Yadav, O. P.; Bachheti, R. K., Photocatalytic Degradation of Methyl Orange Dye using Cr-doped ZnS Nanoparticles under Visible Radiation. *Int. J. Chemtech. Res.* **2013**, *5*, 1452-1461.
3. Rao, H.; Lu, Z.; Liu, X.; Ge, H.; Zhang, Z.; Zou, P.; He, H.; Wang, Y., Visible light-driven photocatalytic degradation performance for methylene blue with different multi-morphological features of ZnS. *RSC Advances*. **2016**, *6(52)*, 46299-46307.
4. Rahdar, A., Effect of 2-mercaptoethanol as capping agent on ZnS nanoparticles: structural and optical characterization. *J. Nanostructur. Chem.* **2013**, *3(1)*, 10.
5. Rahdar1, A.; Aliahmad, M.; Asnaashari, Effect of different capping agents on the undoped ZnS semiconductor nanocrystals :Synthesis and Optical and Structural characterization. *Adv. Sci. Lett.***2013,** *19*, 547-549.
6. Li, J.; Xu, Y.; Liu, Y.; Wu, D.; Sun,Y. Synthesis of Hydrophilic ZnS Nanocrystals and Their Application. *China Particuology.* **2004,** *2*, 266-269.
7. Zhang, X.; Song, H.; Yu, L.; Wang, T.; Ren, X.; Kong, X.; Xie, Y.; Wang, X.; Surface states and its influence on luminescence in ZnS nanocrystallite. *J. Lumin.* **2006**, *118(2)*, 251-256.
8. Wageh, S.; Linga, Z. S.; Rong, X. X., Growth and optical properties of colloidal ZnS nanoparticles. *J. Cryst. Growth.* **2003**, *255*, 332–337.
9. Zhang, H.; Chen, X.; Li, Z.; Kou, J.; Yu, T.; Zou, Z., Preparation of sensitized ZnS and its photocatalytic activity. *J. Phys. D: Appl. Phys.* **2007**, 40, 6846–6849.
10. Sharma, M.; Jain, T.; Singh. S.; Pandey, O. P., Photocatalytic degradation of organic dyes under UV–Visible light using capped ZnS nanoparticles. Sol Energy. **2012**, *86*, 626-633.
11. Khan, M. M. R.; Pal, S.; Hoque, M. M.; Alam, M. R.; Younus, M.; Kobayashi., Simple Fabrication of PVA−ZnS Composite Films with Superior Photocatalytic Performance: Enhanced Luminescence Property, Morphology, and Thermal Stability. *ACS Omega* **2019**, *4*, 6144−6153.

12. Waghadkar, Y.; Arbuj, S.; Shinde, M.; Ballal, R.; Rane, S.; Gosavi, S.; Fouad. H.; Chauhan. R., Hydrothermally Synthesized Zinc Sulphide Microspheres for Solar Light-Driven Photocatalytic Properties. *J. Electron. Mater.* **2018**, *47*, 2687-2693.
13. Kaur, S.; Sharma, S.; Umar, A.; Singh, S.; Mehta, S. K.; Kansal, S. K., Solar light driven enhanced photocatalytic degradation of brilliant green dye based on ZnS quantum dots. *Superlattices and Microstructures*, **2016**, *103*, 365-375.
14. Nachimuthu, S.; Pushpanathan, K.; Cerium Doped ZnS Nanorods for Photocatalytic Degradation of Turquoise Blue H5G Dye. *J. Inorg. Organo. Met. P.* **2019**, *29*, 1141-1153.
15. Chen. F.; Cao. Y.; Jia. D., A facile route for the synthesis of ZnS rods with excellent photocatalytic activity. *Chem. Eng. J.* **2013**, *234*, 223-231.
16. Jaffre, A.; Bregiroux, D.; Reekie, D.; Shears. R., Morphological control of ZnS nanopowders by different capping molecules. *Mater. Lett.* **2017**, *209*, 539-542.
17. Kakarndee, S.; Juabrum, S.; Nanan, S., Low temperature synthesis, characterization and photoluminescence study of plate-like ZnS. *Mater. Lett.* **2016**, *164*, 198-201.
18. Pal, B.; Pal, B., Tuning the optical and photocatalytic properties of anisotropic ZnS nanostructures for the selective reduction of nitroaromatics. *Chem Eng J.***2015**, *263*, 208.
19. Senthilkumar, K.; Ramamurthi, K.; Kalaivani, T.; Balasubramanian, V., Low Temperature Synthesis of MPA Capped ZnS Quantum Dots and its Characterization Studies. *Indian J. Adv. Chem. Sci.* **2013**, *2(1)*, 1-5
20. Jiang, L.; Sun, Y.; Chen, H.; Luo, J.; Zeng, T.; Wei, J.; Liu, L.; Jin, Y.; Jiao, Z.; Sun, X., Synthesis and characterizations of flower-like ZnS and ZnS: Cu2+ nanostructures *Mater. Lett.***2014**, *131*, 82-85.
21. Ahluwalia, S.; Prakash, NT.; Prakash, R.; Pal, B., Improved degradation of methyl orange dye using bio-co-catalyst Se nanoparticles impregnated ZnS photocatalyst under UV irradiation. *Chem. Eng. J.* **2016**, *306*, 1041-1048.

thesis

ORIGINALITY REPORT

3%	1%	2%	2%
SIMILARITY INDEX	INTERNET SOURCES	PUBLICATIONS	STUDENT PAPERS

PRIMARY SOURCES

1	Submitted to Higher Education Commission Pakistan Student Paper	<1%
2	Submitted to Central Queensland University Student Paper	<1%
3	Debabrata Chatterjee. "Redox Reactions of a [RuIII(hedtra)(pz)] Complex with Biochemically Important Reductants: Kinetic, Mechanistic and Antimicrobial Studies", European Journal of Inorganic Chemistry, 02/2012 Publication	<1%
4	www.jmst.org Internet Source	<1%
5	Submitted to 65046 Student Paper	<1%
6	Jalil H Kareem, Andrew P Abbott, Karl S Ryder. "Shifting desulfurisation equilibria in ionic liquid-oil mixtures", Energy & Fuels, 2019 Publication	<1%

Jyotsna

7	eprints-bangaloreuniversity.in Internet Source	<1%
8	Lu, J.. "Direct propylene epoxidation over barium-promoted Au/Ti-TUD catalysts with H"2 and O"2: Effect of Au particle size", Journal of Catalysis, 20070910 Publication	<1%
9	www.archipel.uqam.ca Internet Source	<1%
10	Huang, N.M.. "@c-Ray assisted synthesis of Ni"3Se"2 nanoparticles stabilized by natural polymer", Chemical Engineering Journal, 20090415 Publication	<1%

Exclude quotes	Off	Exclude matches	< 8 words
Exclude bibliography	On